

The Oligocene vertebrate assemblage of Shine Us (Khalium Basin, south western Mongolia)

Gudrun DAXNER-HÖCK^{1,2}, Margarita A. ERBAJEVA^{3,4}, Ursula B. GÖHLICH²,
Paloma LÓPEZ-GUERRERO^{5,6}, Tserendash NARANTSETSEG⁷, Bastien MENNECART^{2,8},
Adriana OLIVER⁶, Davit VASILYAN^{9,10} & Reinhard ZIEGLER¹¹

(with 12 figures and 13 tables)

Manuscript submitted on July 7th 2018,
the revised manuscript on November 3rd 2018.

Abstract

For the first time a very rich and diverse fossil assemblage was described from the Shine Us locality in south western Mongolia. The sample represents floodplain deposits of the Beger Fm., including aquatic and terrestrial fossils such as freshwater ostracods, fishes, gastropods, reptiles, birds, as well as thirty mammal species. The concentrations of disarticulated, mostly fragmentary bones and teeth are interpreted to be accumulations of small floodplain channels. The fossil

¹ Rupertusstraße 16, 5201 Seekirchen, Austria; e-mail: gudrun.hoeck@sbg.at

² Natural History Museum Vienna, Burgring 7, 1010 Vienna, Austria; e-mail: gudrun.hoeck@nhm-wien.ac.at; ursula.goehlich@nhm-wien.ac.at; mennecartbastien@gmail.com

³ Geological Institute, Siberian Branch, Russian Academy of Sciences, Sahianova Str. 6a, 670047 Ulan Ude, Russia; e-mail: erbajeva@ginst.ru

⁴ A.P. Vinogradov Institute of Geochemistry, Siberian Branch, Russian Academy of Sciences, Favorsky Str., 1, 664033, Irkutsk, Russia; e-mail: sinolag@mail.ru

⁵ Universidad Complutense de Madrid, José Antonio Novais s/n, 28040 Madrid, Spain; e-mail: palomalopez@geo.ucm.es

⁶ Geosfera C.B., Calle Madres de la Plaza de Mayo, 228523 Rivas-Vaciamadrid, Madrid, Spain; e-mail: aoliverp5@gmail.com

⁷ Institute of Paleontology and Geology, Mongolian Academy of Sciences, Danzan Str. 3/1, 15169 Ulaanbaatar, Mongolia; e-mail: ts_narangeo@yahoo.com

⁸ Naturhistorisches Museum Basel, Augustinergasse 2, 4001 Bâle, Switzerland; e-mail: mennecartbastien@gmail.com

⁹ Jurassica Museum, Fontenais 21, 2900 Porrentruy, Switzerland; e-mail: davit.vasilyan@jurassica.ch

¹⁰ University of Fribourg, Chemine de Department of Geosciences, University of Fribourg / Freiburg, Chemin du Musée 6, 1700, Fribourg, Switzerland; e-mail: davit.vasilyan@jurassica.ch

¹¹ Staatliches Museum für Naturkunde Stuttgart, Rosenstein 1, 70191 Stuttgart, Germany; e-mail: reinhard.ziegler@smns-bw.de

composition of the Shine Us assemblage SHU-A/1 is broadly in agreement with well-dated mammal faunas of the “*Amphechinus taatsiingolensis* Abundance Zone” (= letter zone C) of the Valley of Lakes. There, radiometric and magnetostratigraphic datings suggest an early late Oligocene age for this Biozone. The estimated age of the Shine Us assemblage (SHU-A/1) is between 26 and 28 million years.

Key words: Oligocene, vertebrates, taxonomy, stratigraphy, Mongolia.

Kurzfassung

Aus der Fundstelle Shine Us im Südwesten der Mongolei wurde erstmals eine reiche und vielfältige fossile Fauna beschrieben. Die Probe repräsentiert Ablagerungen der Beger Formation. Sie umfasst aquatische und terrestrische Fossilien, Süßwasserostracoden und Fische, Schnecken, Reptilien, Vögel, sowie 30 Säugetierarten. Wir interpretieren die Konzentrationen von disartikulierten, meist zerbrochenen Knochen und Zähnen so, dass sie von kleinen Aukanälen zusammengeschwemmt wurden. Die Zusammensetzung der Fossilien aus der Shine Us Fauna SHU-A/1 stimmt weitgehend mit gut datierten Säugetierfaunen der „*Amphechinus taatsiingolensis* Abundance Zone“ (informelle Zone C) aus dem Tal der Gobiseen überein. Dort ergaben radiometrische und magnetostratigraphische Datierungen ein frühes Oberoligozän als Alter der Biozone. Für die Shine Us Fauna (SHU-A/1) nehmen wir ein Alter zwischen 26 und 28 Millionen Jahren an.

Schlüsselwörter: Oligozän, Vertebrata, Taxonomie, Stratigraphie, Mongolei.

Introduction

The Khaliun Basin is a rift basin in south western Mongolia which extends for 70 to 80 km in west-east direction and is flanked by the offshoot of the Khantaishir and Altai mountain ranges towards north and south, respectively. It is connected with the Sharga Basin in the west and the Beger Basin in the east, and is filled by Cenozoic sediments of more than 200 m thickness above a Paleozoic basement (PAUZER *et al.* 1987). The first geologic research of the entire region was carried out during Joint Soviet-Mongolian Geological Expeditions (LISKUN & BADAMGARAV 1977; DEVYATKIN 1981). The Cenozoic sequence was subdivided into three stratigraphic units, the Khantaishir, Beger, and Uush formations. The Khantaishir Fm. was correlated with the Ergelin Dzo Fm. from eastern Mongolia, the Beger Fm. with the Hsanda Gol Fm. from central Mongolia, and the Uush Fm. with the Loh Fm. also from central Mongolia (LISKUN & BADAMGARAV 1977; DEVYATKIN 1981). So far, only scattered fossils were collected from different stratigraphic horizons of the Shine Us strata in the Khaliun Basin. These fossils are stored in the PIN collection in Moscow. The ruminant *Palaeohypsodontus asiaticus* was mentioned from the Oligocene part of the sequence at fossil point Shine-Us 1 of the Beger Fm. (VISLOBOKOVA 1997: fig. 5), and from the Uush Fm. (Miocene part) the ruminant *Amphitragulus* cf. *gracilis* was mentioned from fossil point Shine-Us 2 (VISLOBOKOVA 1997: fig. 5).

Later (1997 and 2001), the locality Shine Us in the the Khaliun Basin (Fig. 1). was visited by our team for short excursions, in order to compare sediment deposition, fossil

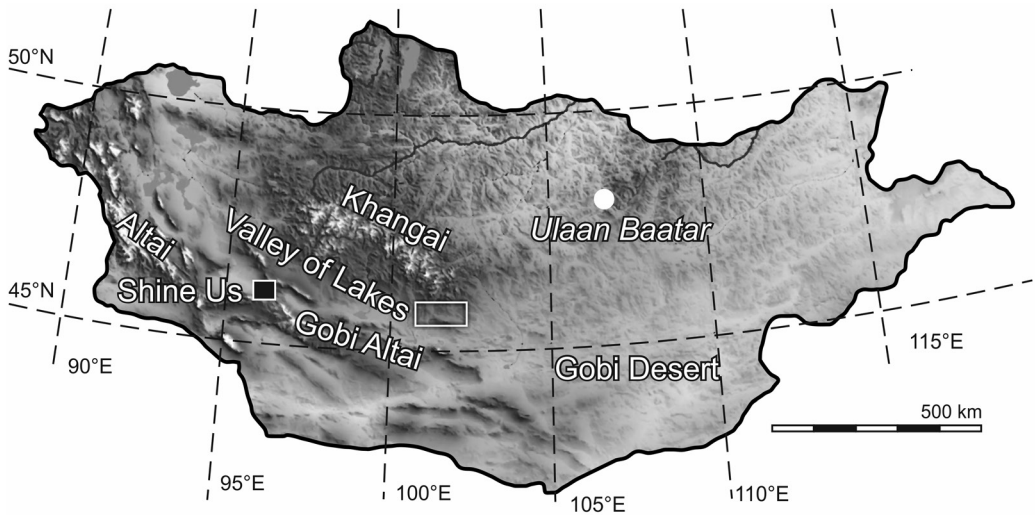


Fig. 1. Topographic map of Mongolia. The position of locality Shine Us in south western Mongolia is indicated by the black square, and the gray rectangle marks the Taatsiin Gol and Taatsiin Tsagaan Nuur localities in the Valley of Lakes. Modified from HARZHAUSER (2016: fig. 1).

content and palaeoenvironmental conditions with the Taatsiin Gol and Taatsiin Tsagaan Nuur region (part of the Valley of Lakes). The latter is located approximately 500 km east of the Khaliun Basin, and that time it was our main study area. The Oligocene and Miocene terrestrial deposits of the Taatsiin Gol and Taatsiin Tsagaan Nuur region are outstanding regarding the rich fossil content and intercalated basalt flows. During eight field-campaigns from 1995 to 2012 we investigated 26 natural outcrops and sections in the course of joint Mongolian-Austrian research projects granted by the Austrian Science Fund (FWF-Projects: P-10505-GEO and P-23061-N19).

The goal of the present paper is to introduce the vertebrate assemblage SHU-A/1 from the Oligocene of Shine Us in the Khaliun Basin. The composition of the small mammal assemblage is very diverse and allows biostratigraphic correlation with some key faunas of the Valley of Lakes. Moreover, although no magnetostratigraphic and radiometric data are available from the Shine Us locality, the integrated studies of the Valley of Lakes region are fundamentals for chronostratigraphic correlation. They also support interpretation of palaeoenvironment and palaeoclimate of the Shine Us locality.

Material and methods

In the course of the above mentioned excursions to Shine Us in the years 1997 and 2001 we collected fossils from the lower part of the Beger Fm., where mammal bones and teeth were imbedded in light brown, locally laminated clayey silt. From one outcrop with visible fossil content we took test samples for wet screening. The total sample size was



Fig. 2. Shine Us locality in the Khaliun Basin, south western Mongolia. The light brown clayey silt correlates with the middle to upper part of layer 17 of the Shine Us section. The white arrow in front marks the sample place of assemblage SHU-A/1. Scattered bones and a palynological sample were also collected from this place (N 46°05'38.2" E 96°04'23.4"; 1683 m elevation) during excursions from 1997, 2001, and 2015. Photo: G. DAXNER-HÖCK, 2015.

no more than 300 kg. Additionally, we collected fossils from the naturally eroded surface of this place within a few square meters. The sample was collected at N 46°05'38.2" E 96°04'23.4" (Fig. 2), north east of the geological section, with its base at N 46°05'35" E 96°04'12.9". The fossil bed yielding assemblage SHU-A/1 can be correlated with the middle to upper part of unit 17 (Beger Fm.) of the logged section (Fig. 3).

The sample was wet-screened in the Valley of Lakes field-camp at Taatsiin Gol. The subsequent process of selecting fossils from the residuals, first identifications, numbering and arranging of fossils was carried out in Austria. Later, the different taxonomic groups were distributed to the co-authors for description. SEM-images were taken by D. GRUBER (Biocenter, University of Vienna), P. VALVERDE and S. FRAILE (Museo Nacional de Ciencias Naturales-CSIC, Madrid), and K. WOLF-SCHWENNINGER (Staatliches Museum für Naturkunde, Stuttgart). The fossils (assemblage SHU-A/1) collected by D. BADAMGARAV† and G. DAXNER-HÖCK (1997 and 2001) are described in the present paper and stored in the collection of the Natural History Museum in Vienna, Austria. Sediment

samples collected for palynological research and some additional small mammal fossils found in the course of later excursions (2009 and 2015), are not included in this study. They are under care of the Mongolian researchers N. ICHINNOROV and B. BAYARMAA from the Palaeontological-Geological Institute of the Mongolian Academy of Sciences, Ulaanbaatar. The composite geological section SHUS1 was studied by D. BADAMGARAV† and T. NARANTSETSEG in 2009, and is herein presented by T. NARANTSETSEG.

Underlines of figure numbers indicate that figured specimens were mirrored (*e. g.*, Fig. 10 A8 shows a right M1, but the M1 is figured as if it were from the left side).

Fossil record: Along with freshwater ostracods, gastropods, fishes, lizards, snakes, and birds, the Shine Us assemblage SHU-A/1 comprises more than 900 mammal remains, which derive from 30 mammal taxa. The fossil collection consists of well-represented taxonomic groups, and also of very rare ones. In the present paper we describe the well-represented fossils in detail (authors in brackets): Lagomorpha (M. ERBAJEVA), Erinaceomorpha, Soricomorpha, and Chiroptera (R. ZIEGLER), Cricetidae (P. LÓPEZ-GUERRERO), Ctenodactylidae (A. OLIVER), Dipodidae (G. DAXNER-HÖCK) and Ruminantia (B. MENNECART). Moreover, the rare remains of Aves (U.B. GÖHLICH), Lacertidae and Serpentes (D. VASILYAN) are presented and figured in this article. Not described are tooth fragments and some strongly worn teeth of the rodent families Sciuridae, Aplodontidae, Eomyidae, and Tsaganomyidae and of the lagomorphs *Desmatolagus*, *Sinolagomys*, and *Archeolagus*. We also omit the freshwater Ostracoda (Cyprididae and Candonidae), egg shells, the few remains of Gastropoda (Pupilloidea / mostly internal casts), and Pisces (Cyprinidae / pharyngeal teeth and vertebrae).

Abbreviations

NHMW collection of the Natural History Museum Vienna, Department of Geology and Palaeontology

AMNH collection of the Natural History Museum, New York

PIN collection of the Paleontological Institute of the Russian Academy of Sciences, Moscow

P – M premolars and molars of the upper dentition

p – m premolars and molars of the lower dentition

I – i upper and lower incisivi

C – c upper and lower canini

D upper deciduous premolar

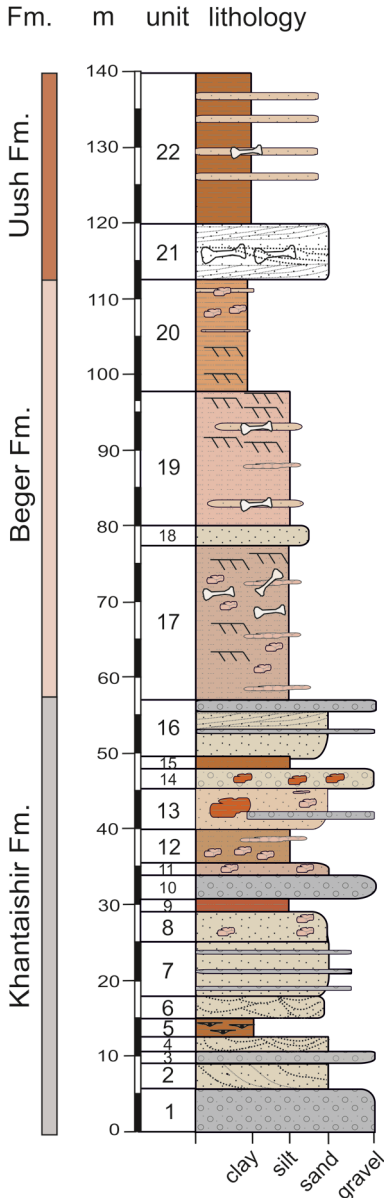
d lower deciduous premolar

n number of specimens

s standard deviation

V variability coefficient

Locality: Shine Us
Section: SHUS1



Legend:

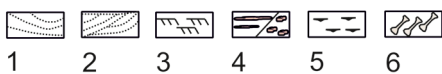


Fig. 3. Detailed stratigraphic column of the Shine Us section (SHUS1) from Shine Us, Khaliun Basin, south western Mongolia, studied by BADAMGARAV[†] and NARANTSETSEG 2009. The base of the section is at: N 46° 05'35"; E 96° 04'12.9". Legend: 1 planar cross bedding, 2 trough cross-bedding, 3 ripple marks, 4 carbonate lenses and concretions, 5 manganese oxide concretions, 6 fossils.

Geological section (T. NARANTSETSEG)

The composite section (SHUS1) of the Shine Us locality was studied by BADAMGARAV and NARANTSETSEG in summer 2009 (Fig. 3). It is placed in the central part of the Khaliun Basin near Shine Us Khudag. The logged section covers parts of the Khantaishir, Beger, and Uush formations and represents a total thickness of 140 m.

The stratigraphic base of the Khantaishir Fm. well crops out at N 46°05'35"; E 96°04'12.9" on top of Paleozoic basement rocks. It consist mainly of light grey gravel, green to yellowish-grey sand, and yellowish brown fine to coarse sand facies intercalating with minor greenish to reddish brown silt and clay layers (Fig. 3; units 1–16). Gravels are mainly subangular to subrounded, up to 25 cm in diameter, poorly sorted, polymict, and without visible textures. Bed thicknesses vary from 1.2 m to 6.4 m. The sand is fine to coarse grained, polymict, and shows horizontal, planar and trough cross-bedding with set thicknesses up to 3.2 m. The sand is generally poorly sorted, but well sorted within the cross beds. Furthermore, the sand contains numerous gravel and cobble-lenses as well as thin layers (up to 40 cm thick). Additional elements include reddish brown clay nodules, well-rounded carbonate concretions up to 20 cm in diameter, and rare manganese oxide concretions. Silt and clays are slightly carbonaceous and mainly show a massive texture,

although rare laminated and spotted textures are present. They also contain rare carbonate concretions and manganese oxide concretions. The total thickness of the Khantaishir Fm. is 56.6 m at the SHUS1 section.

The Beger Fm. (Fig. 3; units 17–20), with a total thickness of 36.1 m, crops out at the weathered surface of the Khantaishir Fm. It consists mainly of bedded reddish brown silt and clay – predominantly in its lowermost part – alternating with beds of yellowish grey fine to coarse sand. The silt- and clay-layers of the middle and upper part are usually thin or ripple laminated and contain abundant carbonate concretions up to 15 cm in size. Numerous fossil remains are included in silt-lenses or clayey silt-layers. The light-brown clayey silt (middle to upper part of unit 17) is partly horizontally laminated, and is distinguished by its fossil richness. The SHU-A/1 assemblage stems from an outcrop of unit 17 (Fig. 2). The sample place is located north east of the logged section, at N 46°05'38.2" E 96°04'23.4".

The Uush Fm. consists of light grey moderately compacted fine-grained sandstone in the lower part (Fig. 3; unit 21), and thick beds of reddish brown silty clay containing numerous layers of yellowish fine sand in the upper part (Fig. 3; unit 22). The basal sandstone shows well-preserved planar and trough cross-bedding textures, and contains a pinkish grey thin carbonate layer about 3–4 cm in thickness. Fossil remains occur in the sandstone. The sandstone suggests the change from Oligocene to Miocene deposits. The total thickness of the Uush Formation is 27.7 m.

Systematic Palaeontology

Squamata and Serpentes (D. VASILYAN)

Class Reptilia LAURENTI, 1768

Order Squamata OPPEL, 1811

Family Lacertidae OPPEL, 1811

Lacertidae indet.

(Fig. 4 A)

Material: three incomplete dentaries (NHMW 2018/0040/0001–0003) from sample SHU-A/1.

Description and comments: The dentary fragments exhibit sharp small-sized bicuspid teeth, with a large central cusp and a smaller lateral one. The lingual surface of teeth is smooth. The preserved lamina horizontalis is rather low and has a flat lingual surface. Based on the presence of bicuspid teeth, all available specimens can be attributed

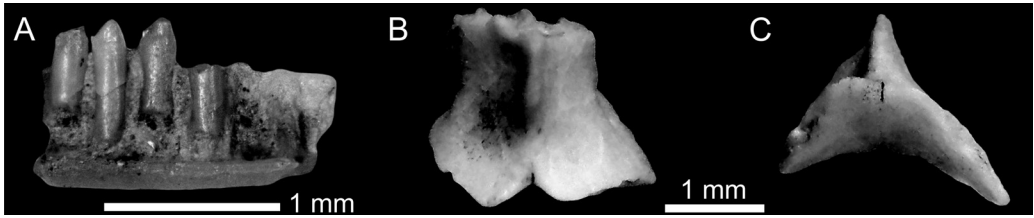


Fig. 4. Squamates from the Shine Us locality (assemblage SHU-A/1), Khaliun Basin, south western Mongolia, Beger Fm., late Oligocene. A. Lacertidae indet., dentary NHMW 2018/0040/0001) in lingual view, and B–C. Serpentes indet., neural arch (NHMW 2018/0041/0001) in dorsal and anterior views.

to small-sized lizards of the family Lacertidae (KOSMA 2004). The presence of lizards in the material suggests the availability of open (rocky) habitats where the sunlight reaches the ground.

Suborder Serpentes (LINNAEUS, 1758)

Serpentes indet.

(Fig. 4 B–C)

Material: one fragmentary neural arch (NHMW 2018/0041/0001).

Description and remarks: The roof of the neural arch is preserved. It shows a low and short neural crest which does not reach the anterior margin of the neural arch. The zygospine is rather well-developed. The morphology of the neural arch resembles that of the snakes (HOFFSTETTER & GASC 1969) but no precise identification is possible.

Aves (U.B. Göhlich)

Class Aves LINNAEUS, 1758

Aves indet.

A very few and extremely fragmentary bird bones (NHMW 2018/0135/0000) were present in the screen washing residue of the Shine Us sediments, but they allow no precise systematic assignment.

Order Accipitriformes VIEILLOT, 1816

Family Accipitridae, VIEILLOT, 1816

Accipitridae indet.
(Fig. 5 A–D)

Material and measurements: Best preserved is an almost complete claw (NHMW 2018/0135/0001), which represents a diurnal bird of prey. It is 16 mm in length; the estimated complete length was about 18 mm. Height and width of the cotyla articularis are 6.6×5 mm.

Description: The claw is almost complete and lacking only the outermost tip (apex). It can be identified as an accipitrid claw due to the very strong tuberculum flexorium (apophysis flexoris) and the flattened plantar side of the corpus phalangis. The concave proximal cotyla articularis is pyriform in outline and relatively symmetrically subdivided in two halves. The tuberculum flexorium is strongly developed, projecting plantoapically and terminating in a bulky knob; a foramen, topped by a thin crest running plantoapically, is located laterally on both sides of the basis of the tuberculum flexorium.

Discussion: Not many fossils of diurnal birds (Accipitriformes) are known from the Oligocene or lower Miocene of Mongolia or Central Asia. KUROCHKIN (1968a) described three accipitrid species from the Oligocene of Mongolia: “*Buteo*” *circoides* KUROCHKIN, 1968a (distal ulna), *Venerator (Tutor) dementjevi* (KUROCHKIN, 1968a) (distal humerus), and *Gobihierax edax* KUROCHKIN, 1968a (distal humerus) (for more information see KUROCHKIN *et al.* 2015; MAYR 2009). KUROCHKIN (1968b, 1976) further mentioned several femora resembling the recent Aegypiinae (Old World vultures) from the lower Oligocene of Mongolia, and an accipitrid (“*Aquilavus*”) from the upper Oligocene of Kazakhstan. Furthermore, OLSON (1985) pointed to undescribed Cathartidae (New World vultures) from the lower Oligocene of Mongolia. Lower Miocene bird fossils are very poorly investigated throughout Asia. No diurnal bird material is described so far from the lower Miocene of Central Asia. The lower and middle Miocene of eastern Asia (ZELENKOV 2016), however, have yielded the vultures *Qiluornis taishanensis* HOU *et al.*, 2000 (partial hindlimb) and *Mioaegypius gui* HOU, 1984 (tarsometatarsus).

Almost none of the above-mentioned taxa are represented by claw(s), preventing comparisons with the present claw from Shine Us. Only claws of *Qiluornis taishanensis* are described, but clearly differ from the Shine Us claw by reduced tubercula flexorii and extensorii (MANEGOLD *et al.* 2014).

Own comparisons with claws of extant accipitrids and falconiforms, namely *Falco cherrug cyanopus*, *Coragyps atratus brasiliensis*, *Pandion haliaetus*, *Pernis apivorus*, *Gypaetus barbatus*, *Buteo buteo*, *Nisaetus cirrhatu*s, *Aquila chrysaetos*, *Milvus milvus*, *Accipiter gentilis*, and *Haliaeetus albicilla* (all comparative material housed in the ornithological collection of the NHMW), show that the Shine Us claw clearly differs morphologically from Falconiformes, Cathartidae, and Pandionidae. Within the compared Accipitridae, the claw most closely resembles those of *Buteo buteo*, especially in the size and shape of the tuberculum flexorium. In its dimension the claw corresponds to those of digit I and II of a female *Buteo buteo* (e. g., NHMW-Zoo1 11.019); accordingly,

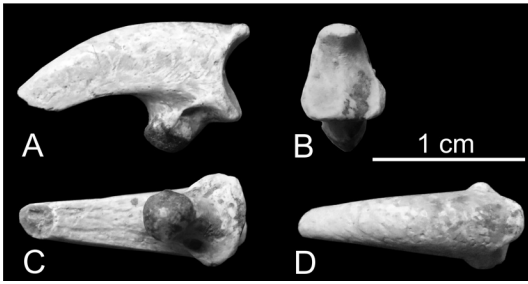


Fig. 5. Pedal claw (probably of digit I or II) (NHMW 2018/0135/0001) of an accipitrid bird in A. lateral, B. proximal, C. plantar, and D. dorsal view. Shine Us locality (assemblage SHU-A/1), Khaliun Basin, south western Mongolia, Beger Fm., upper Oligocene.

the accipitrid taxon to which the claw belongs had an estimated body mass of about 1 kg. However, the presence of only one claw does not allow a more precise systematic determination.

Based on the described vertebrate fauna from Shine Us, this bird of prey had a diverse choice of prey animals including small mammals and reptiles.

Lagomorpha (M.A. ERBAJEVA)

Dental terminology after LOPEZ MARTINEZ (1989).

Class Mammalia LINNAEUS, 1758

Order Lagomorpha BRANDT, 1855

Family Ochotonidae THOMAS, 1897

Subfamily Sinolagomyinae GUREEV, 1960

Genus *Bohlinotona* DE MUIZON, 1977

Bohlinotona cf. pusilla (TEILHARD DE CHARDIN, 1926)

(Fig. 6 A–G, Tab. 1)

1926 *Desmatolagus pusillus* n. sp., pro parte – TEILHARD DE CHARDIN: 23, figs 11 A, B, 12 B.

1977 *Bohlinotona pusilla* (TEILHARD DE CHARDIN, 1926), pro parte – DE MUIZON: 272, fig. 3 b, c, d.

1998 *Bohlinotona pusilla* (TEILHARD DE CHARDIN, 1926) – ERBAJEVA & SEN: 98, figs 2–3, tab. 1.

Material (inv. numbers): 1 p3 (NHMW 2013/0113/0001), 1 m2 (NHMW 2013/0113/0002), 1 P2 (NHMW 2013/0113/0003), 1 P3 (NHMW 2013/0113/0004), 1 P4 (NHMW 2013/0113/0005), 3M1 (NHMW 2013/0113/0006–0008, 2013/0113/0010), 1 M2 (NHMW 2013/0113/0009), 1 p4–m1 (NHMW 2013/0113/0016), 1 p3–m2 (NHMW 2013/0113/0017), 1 p4–m2 (NHMW 2013/0113/0018), 1 P3–P4 (NHMW 2013/0113/0020), 1 P3–M1 (NHMW 2013/0113/0021), 3 D4 (NHMW 2013/0113/0011–0013), 1 d3 (NHMW 2013/0113/0014), 1 incisor (NHMW 2013/0113/0015), 1 fragment

of m1 trigonid (NHMW 2013/0113/0019). Additionally, 200 molars, premolars, and deciduous teeth (NHMW 2013/0113/0020–0220), and many tooth fragments and incisors (NHMW 2013/0113/0000) were recently selected from the remaining part of residuals. These additional fossils will be published in another context.

Measurements: see Tab. 1.

Description: Small-sized hypsodont teeth. Except for P2 the upper teeth are transversely curved and have three roots, *i. e.*, two short small lateral roots and a large permanently growing internal root. The internal root of old individuals can even form a circle. Accordingly, the occlusal surface of strongly worn teeth is very wide.

P2: The tooth is column shaped, slightly curved and has one root. The occlusal surface is oval. Two shallow anterior reentrants (paraflexus) extend to the root and are filled with a small amount of cement (Figs 6 B1, 6 B2).

P3 of young individuals have an oval occlusal outline, with three cones separated by anterior reentrants. The deep internal reentrant is filled with cement, the shallow external lacks cement (Figs 6 D1, 6 D2). The internal cone (protocone) has an anteroloph, the large middle one (paracone) is bulbous in outline, the external one (metacone) is smallest and very short. The lingual margin of P3 shows no trace of the hypostria. Worn teeth gradually become wider. The anteroloph and the lingual part of the paracone are separated by the internal reentrant but stay in place (Fig. 6 A).

Table 1. Descriptive statistics of tooth measurements of *Bohlinotona cf. pusilla* from assemblage SHU-A/1, locality Shine Us, Khaliun Basin, south western Mongolia.

	length (mm)			width (mm)	
	range	mean	n	range	mean
P3–M1		3.50	1		
P3–P4	2.25–2.35	2.30	2		
P2		0.65	1		
P3	1.00–1.25	1.08	3	1.90–3.70	2.60
P4	1.10–1.20	1.13	3	2.15–4.70	3.15
M1	1.10–1.25	1.15	3	2.60–4.25	3.40
M2		1.00	1		
p3–m2		4.85	1		
p3–m1		3.50	1		
p3–p4		2.15	1		
p4–m1	2.65–2.90	2.76	2		
p3		0.95	2	1.10–1.20	1.15
p4	1.35–1.45	1.40	3	1.50–1.60	1.53
m1	1.35–1.50	1.42	3	1.50–1.70	1.60
m2	1.40–1.50	1.43	3	1.40–1.60	1.50

P4: The tooth is rectangular in occlusal outline (Fig. 6 D1), relatively long externally, and shorter internally. The enamel band is well developed at the anterior and lingual margins, it is absent at the external and posterior ones. Teeth of young individuals have a crescentic valley filled with cement. The cement disappears in advanced wear stages. The internal border gradually becomes sharp, the lateral margin remains relatively straight (Fig. 6 A).

Worn M1 and M2 show a similar trend, although M2 has slightly sharper internal and external edges. Moreover, the anterior margin of M2 is wider than the posterior one (Figs 6 C1, 6 C2).

The mandible is relatively robust below p4. The lower incisor extends posteriorly as far as the end of m1, developing a visible tubercle on the lingual and labial sides of the mandibular ramus. The foramen mentale is located below p3.

The p3 is triangular in occlusal outline, has smooth rounded edges, and the antero-external fold is filled with a small amount of cement (Figs 6 E, 6 F1–F4). The posterior border of p3 is straight. The entire tooth crown is covered by enamel.

The p4–m2 have sharp external and rounded internal edges. The enamel band is well developed on the external and posterior margins of the trigonid and talonid. The trigonid and talonid are connected by cement, with the former being wider than the latter. Externally the trigonid is longer because of its convex anterior and posterior borders. The talonid is oval with a sharp external edge (Figs 6 E, 6 G), (Tab. 1).

The m3 was not found yet, but the mandible displays a round alveola for m3.

Discussion: The Ochotonidae species *B. pusilla* was first evidenced from the locality Saint-Jacques in China. Originally, the fossils were described as *Desmatolagus pusillus* by TEILHARD DE CHARDIN (1926). Later, DE MUIZON (1977) referred the species to a new genus, *Bohlinotona* DE MUIZON, 1977. The re-examinations of the Saint-Jacques material by ERBAJEVA & SEN (1998) revealed that the type material of *B. pusilla* included two genera and two species, the type species *Bohlinotona pusilla* (TEILHARD DE CHARDIN, 1926) and *Desmatolagus chinensis* ERBAJEVA & SEN, 1998.

Bohlinotona cf. *pusilla* is also known from the upper Oligocene of Mongolia (letter zones C and C1), from the localities Toglорhoi (TGW- A/2), Taatsiin Gol (TGR-C/1+2), Unzing Churum (TAR-A/2), Del (DEL-B/12), and Huch Teeg (RHN-A/9) (ERBAJEVA 2007; ERBAJEVA & DAXNER-HÖCK 2014). The SHU-A/1 assemblage comprises four Lagomorpha taxa, the Ochotonidae *B. cf. pusilla* and *Sinolagomys* sp., and the Leporidae *Archaeolagus* sp. and *Desmatolagus* sp. While *B. cf. pusilla* is well represented by upper and lower jaw-fragments, isolated premolars, molars, deciduous teeth, incisors and numerous tooth-fragments, the other three taxa are poorly evidenced by only 1–2 specimens each: 1 P3 and I sup. of *Sinolagomys* sp. (NHMW 2013/0382/0001 and 0002), 1 M1 of *Archaeolagus* sp. (NHMW 2013/0171/0001) and m1–m2 of *Desmatolagus* sp. (NHMW 2013/0172/0001). The latter three taxa and the deciduous teeth of *Bohlinotona* are not described in detail here.

Bohlinotona cf. *pusilla* from Shine Us resembles the nominative species from the locality Saint-Jacques in China, but it differs slightly from the type material by its smaller size

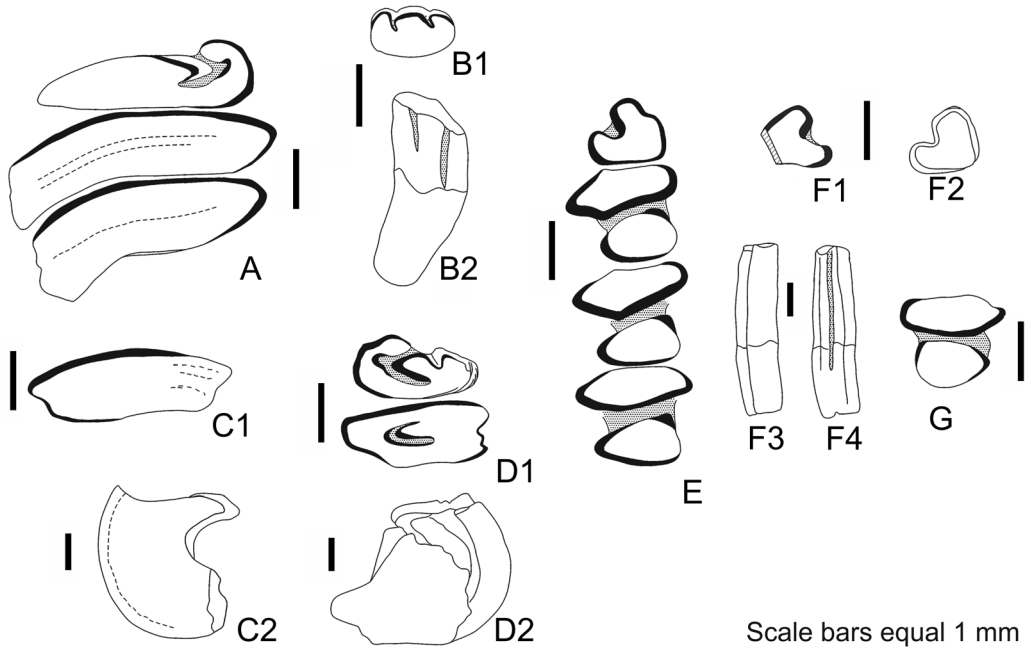


Fig. 6. *Bohlinotona cf. pusilla* (TEILHARD DE CHARDIN, 1926) from the Shine Us locality (assemblage SHU-A/1) in the Khaliun Basin, south western Mongolia, Beger Fm., upper Oligocene. **A**: right P3-M1 (NHMW 2013/0113/0021); **B1**: left P2 (NHMW 2013/0113/0003), occlusal view, **B2**: left P2 frontal view; **C1**: left M2 (NHMW 2013/0113/0009), occlusal view; **C2**: left M2, posterior view; **D1**: left P3-P4 (NHMW 2013/0113/0020), occlusal view, **D2**: left P3-P4, frontal view; **E**: left p3-m2 (NHMW 2013/0113/0017); **F1**: right p3 (NHMW 2013/0113/0001), occlusal view, **F2**: right p3, view from bottom of tooth, **F3**: right p3, frontal view, **F4**: right p3, lateral view; **G**: right m2 (NHMW 2013/0113/0002).

and a wider and shorter talonid. These minor differences may reflect individual variability or regional differences of *B. pusilla*. All four genera – *Bohlinotona*, *Sinologomys*, *Archaeolagus*, and *Desmatolagus* – are also characteristic elements of the Saint-Jacques fauna, dated as upper Oligocene.

Erinaceomorpha, Sciuromorpha and Chiroptera (R. ZIEGLER)

Dental terminology after ENGESSER (1980) for erinaceids, REUMER (1984) for soricids, HUTCHISON (1974) for talpids, and SIGÉ (1968) for chiropterans.

Order Erinaceomorpha GREGORY, 1910

Family Erinaceidae FISCHER VON WALDHEIM, 1817

Subfamily Brachyericinae BUTLER, 1948

Brachyericinae gen. et sp. indet.

(Fig. 7 A)

Material (state of preservation allows no measurements): Left edentulous dentary fragment (NHMW 2018/0021/0001).

Description and remarks: The mental foramen is situated below the alveolus, anterior to the p4 alveolus. The strong masseteric ridge extends to below p4. That ridge is a distinctive character of Brachyericinae. The species of this subfamily differ in size, the number of premolars, the position of the mental foramen, and in the degree of sculpturing of the buccal sides of p4–m2. The specimen is quite similar to *Exallerix pustulatus* ZIEGLER *et al.*, 2007 from the Hsanda Gol Fm. at the Taatsiin Gol locality, but differs from it in the more anterior location of the mental foramen. A more precise identification of the specimen is not possible.

Subfamily Erinaceinae FISCHER VON WALDHEIM, 1817

Genus *Palaeoscaptor* MATTHEW & GRANGER, 1924

***Palaeoscaptor cf. rectus* MATTHEW & GRANGER, 1924**

(Fig. 7 B)

1924 *Palaeoscaptor rectus* new species. – MATTHEW & GRANGER: 3.

1970 *Ampechinus (Palaeoscaptor) cf. rectus* (MATTHEW & GRANGER, 1924) – SULIMSKI: 63, pl. XIX, fig. 4, text-fig. 1A, C.

1984 *Ampechinus rectus* MATTHEW & GRANGER, 1924 – HUANG: 306–308, pl. 1, figs 4–11.

1984 *Ampechinus cf. rectus* MATTHEW & GRANGER, 1924 – HUANG: 308, pl. 1, fig. 1.

2007 *Palaeoscaptor cf. rectus* MATTHEW & GRANGER, 1924 – ZIEGLER, DAHLMANN & STORCH: 83 f., fig. 8.

Material and measurements: three specimens; right m1 (NHMW 2018/0022/0001), length 3.85 mm, anterior width 1.97 mm, posterior width 2.05 mm; right m2-trigonid (NHMW 2018/0022/0002) anterior width 1.91 mm; left m1-talonid (NHMW 2018/0022/0003) posterior width 2.00 mm.

Remarks: The only nearly complete tooth, a left m1, shows the elongated trigonid, which is the apomorphic feature of the genus *Palaeoscaptor*. The protoconid is partly broken off. The tooth is distinctly larger than the m1 of *P. acridens* MATTHEW & GRANGER, 1924. Nonetheless, it is also much smaller than in *P. gigas* (LOPATIN, 2002). The specimen best fits with *P. rectus* from several Oligocene localities in the Valley of Lakes (see measurements in ZIEGLER *et al.* (2007: tabs 5, 7, p. 90)).

***cf. Palaeoscaptor gigas* (LOPATIN, 2002)**

(Fig. 7 C)

2002 *Ampechinus gigas* sp. nov. – LOPATIN: 303, fig. 1.

2007 *Palaeoscaptor gigas* (LOPATIN, 2002) – ZIEGLER, DAHLMANN & STORCH: 88 f., fig. 9.

Material and measurements: three specimens; left m1 paracristid (NHMW 2018/0023/0001), length 3.71 mm; right m1 paracristid (NHMW 2018/0023/0002), length 3.64 mm; left P3-fragment (NHMW 2018/0023/0003), width 1.46 mm.

Description: The long paracristid shows that the trigonid of the m1 was elongated, which is characteristic of Brachyerincinae and *Palaeoscaptor*. The fragment sizes correspond well with *P. gigas*. Due to the absence of tubercles they cannot belong to *Exallex* MC KENNA & HOLTON, 1967. The postparacrista of P3 is broken off. There is no distinct parastyle.

Table 2. *Ampechinus taatsiingolenis*, sample statistics of the teeth. (measurements in mm, n = number of specimens, s = standard deviation, V = coefficient of variation).

	n	range	mean	s	V
d4 width	2	0.69–0.97	0.83		
p4 length	6	1.30–1.40	1.34	0.041	3.09
p4 width	10	0.77–0.88	0.84	0.041	4.92
m1 length	10	1.83–2.14	1.96	0.094	4.81
m1 width anterior	16	1.00–1.18	1.10	0.050	4.60
m1 width posterior	17	0.97–1.70	1.15	0.077	6.71
m2 length	8	1.45–1.62	1.55	0.060	3.91
m2 width anterior	11	0.93–1.10	1.02	0.052	5.13
m2 width posterior	8	0.87–1.04	0.96	0.053	5.46
m3 length	9	0.74–0.94	0.83	0.078	9.43
m3 width anterior	10	0.50–0.60	0.56	0.035	6.36
D3 length	2	1.03–1.07	1.05		
D3 width	2	0.77–0.84	0.81		
P3 length	2	1.17–1.19	1.18		
P3 width	1		0.95		
P4 length	1		1.73		
P4 width	2	1.54–1.57	1.56		
M1 length buccal	6	1.59–1.79	1.67	0.077	4.62
M1 length lingual	12	1.35–1.62	1.50	0.084	5.61
M1 width anterior	8	1.74–2.20	1.98	0.139	7.05
M1 width posterior	5	1.83–2.19	2.04	0.144	7.04
M2 length buccal	7	1.11–1.46	1.29	0.110	8.52
M2 length lingual	11	0.92–1.18	1.09	0.076	7.00
M2 width anterior	10	1.54–1.93	1.69	0.124	7.39
M2 width posterior	9	1.31–1.52	1.43	0.078	5.48

Genus *Amphechinus* AYMARD, 1850***Amphechinus taatsiingolensis* ZIEGLER, DAHLMANN & STORCH, 2007**

(Fig. 7 D1–D10, Tab. 2)

2007 *Amphechinus taatsiingolensis* nov. spec. – ZIEGLER, DAHLMANN & STORCH: 96 f, fig. 11.

Material: 92 isolated teeth, partly fragments (NHMW 2018/0024/0001–0092).

Measurements: see Tab. 2 (p. 209).

Description and remarks: Several single-rooted, unicuspid Erinaceidae teeth may be the i3 and lower canines (c) of *Amphechinus*.The p4 have a paraconid as high as the protoconid, a metaconid attached to the lingual face of the protoconid, a marked postcrisid and a faint ectocingulid. The m1 shows the relatively compressed trigonid, characteristic of *Amphechinus*. All m3 are single-rooted and have no talonid, which is an autapomorphy of *Amphechinus*. Five specimens show a weak postcingulid, four m3 none.

The D3, P3 and P4 have a faint protocone and parastyle. In the M1 and M2 a metaconule is, if present at all, a thickening of the end of the postmetaconule crest.

All tooth sizes fit best with *A. taatsiingolensis*. The wide range of some measurements suggests that the sample is inhomogeneous. Some specimens may belong to *Palaeoscaptor*.The larger specimens overlap in size with the smaller teeth of *A. major* (ZIEGLER *et al.* 2007: tabs 5, 9, 11), but the vast majority of the teeth belongs to *A. taatsiingolensis*.

The species is very abundant in assemblages of letter zone C in the Valley of Lakes, but also sporadically occurs up to the Miocene letter zone D.

Order Soricomorpha GREGORY, 1910

Family Soricidae FISCHER, 1814

Subfamily Crocidosoricinae REUMER, 1987

Crocidosoricinae gen. et sp. indet.

(Fig. 7 E)

Material and measurements: four specimens: right m1 (NHMW 2018/0025/0001), length 1.11 mm, anterior width 0.66 mm, posterior width 0.69 mm; left I sup. (NHMW 2018/0025/0002), length 0.97 mm, talon length 0.43 mm, height 0.77 mm; right I sup. (NHMW 2018/0025/0003), length 0.98 mm, talon length 0.48 mm, height 0.74 mm; right M1 (NHMW 2018/0025/0004), labially damaged, no measurements.

Description and remarks: No vestige of pigmentation is preserved on the teeth.

The m1 has a wide postentoconid valley and a marked pre- and postcingulid. The latter extends labially below the hypoconid and continues to below the protoconid. The upper incisors are not fissident and are generalized crocidosoricine upper incisors. In the M1 the parastyle is broken off, and the mesostyle is confluent at moderate wear. The heel is short.

The teeth lumped together here do not necessarily belong to one species. They show the overall crocidosoricine morphology but do not fit with any species recorded by ZIEGLER *et al.* (2007) from the Taatsiin Gol region (Valley of Lakes, Mongolia). They cannot be identified more precisely.

Family Talpidae FISCHER VON WALDHEIM, 1817

Talpidae gen. et. sp. indet.

(Fig. 7 F)

Material and measurements: two specimens; left dentary fragment with m3 (NHMW 2018/0026/0001), length 1.00 mm, width 0.57 mm; right m3-trigonid (NHMW 2018/0026/0002), width anterior 0.55 mm.

Description and remarks: The m3 has a marked precingulid, no further cingulids and no entostylid. The oblique cristid ends at the rear basis of the tigonid, roughly in the middle.

The m3 is distinctly smaller than in *Mongolopala tathue* ZIEGLER, DAHLMANN & STORCH, 2007 and also differs from this species in the oblique cristid terminating more labially. The m3 does not fit with any Talpidae gen. et sp. indet. 1–9, which have been recorded from the Valley of Lakes (see ZIEGLER *et al.* 2007).

As a rule most talpids cannot be identified to species level based solely on the m3.

Order Chiroptera BLUMENBACH, 1779

Family Vespertilionidae GRAY, 1821

Genus *Myotis* KAUP, 1829

cf. *Myotis horaceki* ZIEGLER, 2000

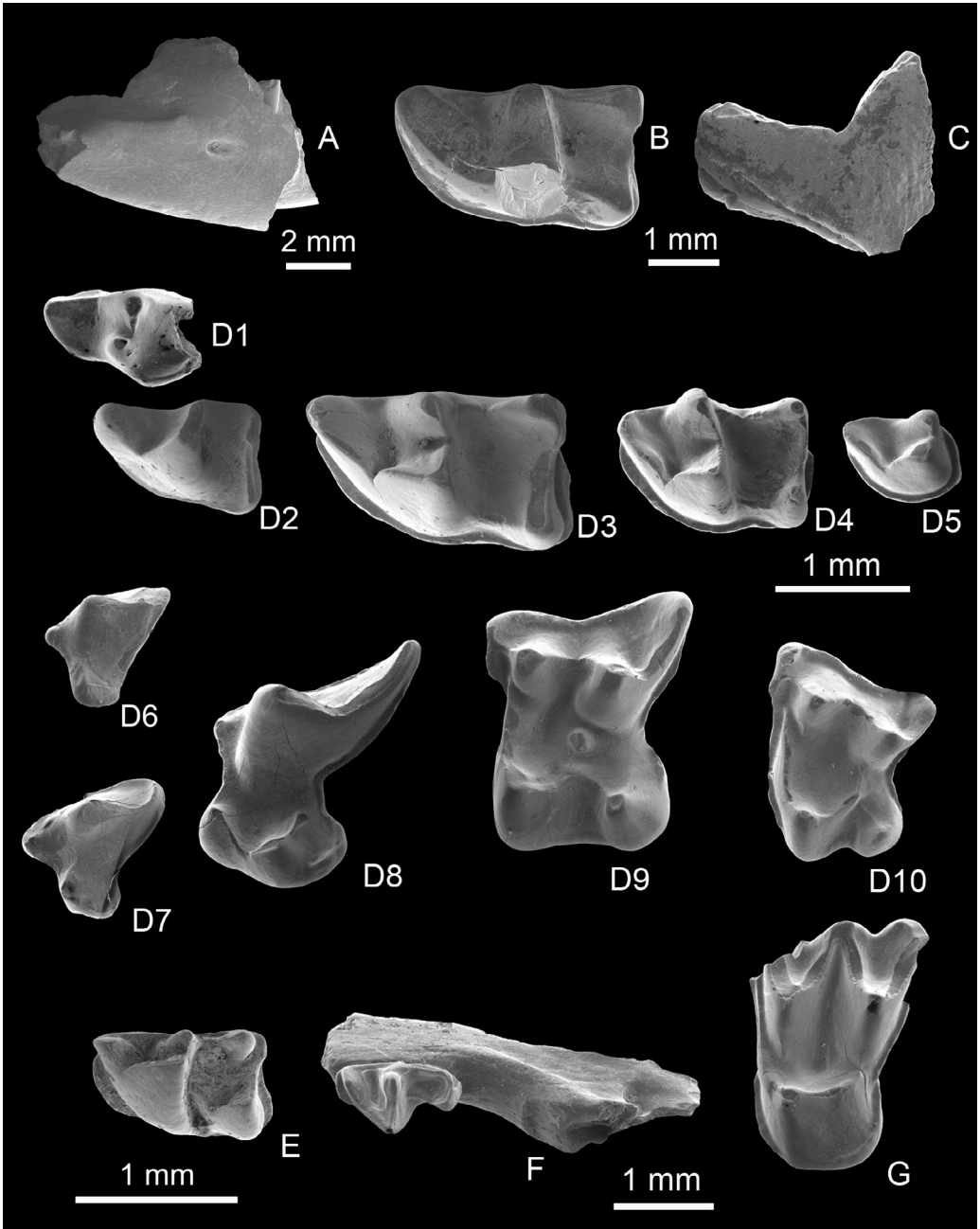
(Fig. 7 G)

2000 *Myotis intermedius* n. sp. – ZIEGLER: 662 f., pl. 6, figs 55–67.

2003 *Myotis horaceki*. – ZIEGLER: 2.

Material and measurements: one specimen: right M2 (NHMW 2018/0027/0001), length 1.50 mm, width 1.96 mm.

Description and remarks: In the right M2, the parastyle is broken off. The tooth has neither hypocone, nor para- and metaconule. No para- and metaloph is developed.



Preprotocrista joins parastyle, postprotocrista ends at the basis of metacone. At moderate wear mesostyle is confluent. Precingulum is faint and restricted to below the mesial basis of protocone. Postcingulum is stronger and broken off near metastyle.

So far no bats are known from the Valley of Lakes sites. Due to the absence of para- and metaloph and the confluent mesostyle, the M2 cannot belong to *Stehlinia* (cf. fig. 16, and diverse species of *Stehlinia* figured in MAITRE 2014). Morphologically the M2 best fits with *Myotis horaceki* (ZIEGLER, 2000) from the upper Oligocene of southern Germany. It is in the uppermost size range of this species.

Ctenodactylidae (A. OLIVER)

For dental terminology see OLIVER & DAXNER-HÖCK (2017: fig. 2).

Order Rodentia BOWDICH, 1821

Family Ctenodactylidae ZITTEL, 1893

Genus *Tataromys* MATTHEW & GRANGER, 1923

***Tataromys sigmodon* MATTHEW & GRANGER, 1923**

(Fig. 8 A1–A7, Tab. 3)

1923 *Tataromys sigmodon* – MATTHEW & GRANGER: 6.

1997 *Tataromys sigmodon* MATTHEW & GRANGER, 1923 – WANG: 18–20, figs 12–14, 41, tabs 4–5.

2006 *Tataromys sigmodon* MATTHEW & GRANGER, 1923 – VIANEY-LIAUD *et al.*: 124–132, figs 6–8, tabs 4–11, pls 1–3.

2017 *Tataromys sigmodon* MATTHEW & GRANGER, 1923 – OLIVER *et al.*: 56, fig. 3.

Material: 133 specimens; 8 D4 left (NHMW 2017/0018/0001–0008), 9 D4 right (NHMW 2017/0018/0009–0017), 10 P4 left (NHMW 2017/0018/0018–0027), 4 P4 right (NHMW 2017/0018/0028–0031), 8 M1 left (NHMW 2017/0018/0032–0039), 7 M1 right

- ◀ Fig. 7. Erinaceomorpha, Soricomorpha, and Chiroptera from the Shine Us locality (assemblage SHU-A/1), Khaliun Basin, south western Mongolia, Beger Fm., upper Oligocene. **A:** Brachyercinae gen. et sp. indet., left dentary fragment (NHMW 2018/0021/0001); **B:** *Palaeoscpator* cf. *rectus*, right m1 (NHMW 2018/0022/0001); **C:** cf. *Palaeoscpator gigas*, left m1 paracristid (NHMW 2018/0023/0001); **D1:** *Amphechinus taatsiingolensis*, left d4 (NHMW 2018/0024/0011); **D2:** *Amphechinus taatsiingolensis*, left p4 (NHMW 2018/0024/0001); **D3:** *Amphechinus taatsiingolensis*, left m1 (NHMW 2018/0024/0013); **D4:** *Amphechinus taatsiingolensis*, right m2 (NHMW 2018/0024/0040); **D5:** *Amphechinus taatsiingolensis*, left m3 (NHMW 2018/0024/0047); **D6:** *Amphechinus taatsiingolensis*, left D3 (NHMW 2018/0024/0061); **D7:** *Amphechinus taatsiingolensis*, right P3 (NHMW 2018/0024/0058); **D8:** *Amphechinus taatsiingolensis*, right P4 (NHMW 2018/0024/0054); **D9:** *Amphechinus taatsiingolensis*, left M1 (NHMW 2018/0024/0063); **D10:** *Amphechinus taatsiingolensis*, right M2 (NHMW 2018/0024/0082); **E:** Crocidosoricinae gen. et sp. indet., right m1 (NHMW 2018/0025/0001); **F:** Talpidae gen. et sp. indet., left dentary fragment with m3 (NHMW 2018/0026/0001); **G:** cf. *Myotis horaceki* ZIEGLER, 2000, right M2 (NHMW 2018/0027/0001).

(NHMW 2017/0018/0040–0046), 7 M2 left (NHMW 2017/0018/0049–0055), 3 M2 right (NHMW 2017/0018/0057–0059), 8 M3 left (NHMW 2017/0018/0060–0067), 3 M3 right (NHMW 2017/0018/0068–0070), 1 fragmentary maxilla with M1–2 right (NHMW 2017/0018/0047), 1 fragmentary maxilla with M1–3 right (NHMW 2017/0018/0048), 1 fragmentary maxilla with M2–3 left (NHMW 2017/0018/0056), 9 d4 left (NHMW 2017/0018/0071–0079), 11 d4 right (NHMW 2017/0018/0080–0090), 5 p4 left (NHMW 2017/0018/0091–0095), 5 p4 right (NHMW 2017/0018/0096–0100), 3 m1 left (NHMW 2017/0018/0101–0102, 2017/0018/0131), 11 m1 right (NHMW 2017/0018/0103–0111, 2017/0018/0132–0133), 3 m2 left (NHMW 2017/0018/0112–0113, 2017/0018/0125), 7 m2 right (NHMW 2017/0018/0114–0120), 4 m3 left (NHMW 2017/0018/0121–0124), 5 m3 right (NHMW 2017/0018/0126–0130).

Measurements: see Tab. 3.

Description: D4: The labial anteroloph is always present and the ingual anteroloph is absent. Commonly the anterior protoloph is present, but in one specimen it is transverse and in another it is posterior. The direction of metaloph varies between backwards, transverse and anterior.

P4: The labial anteroloph is very diverse, it is long, medium, short, incipient or absent. The lingual anteroloph is absent. The labial posteroloph is always present and it is long, medium or short. The lingual posteroloph is long and connected to the protocone, it is short, incipient or absent.

M1: The labial anteroloph is always present and usually of medium length. The lingual anteroloph is absent except in two specimens. An anterior protoloph is present, except in one tooth where it is transverse. The metaloph points backwards, transversely or forwards.

Table 3. Descriptive statistics of *Tataromys sigmodon* from Shine Us. Abbreviations: n = number of teeth measured.

	length (mm)			width (mm)	
	range	mean	n	range	mean
D4	1.74–2.01	1.87	8/9	1.61–2.31	1.92
P4	1.44–1.84	1.67	12/11	1.78–2.35	2.14
M1	2.14–2.51	2.34	14/16	1.68–2.36	2.18
M2	2.63–2.88	2.74	9/10	2.32–2.74	2.52
M3	2.46–2.98	2.80	8/9	2.28–2.59	2.46
d4	1.93–2.33	2.09	9/11	1.32–1.57	1.40
p4	1.72–2.03	1.95	8/8	1.32–1.67	1.56
m1	2.49–2.79	2.66	6/9	1.67–2.10	1.89
m2	3.00–3.28	3.14	8/9	2.21–2.40	2.31
m3	3.17–3.41	3.29	2/4	2.35–2.50	2.42

M2: The labial anteroloph is long or medium. A lingual anteroloph is absent. Protoloph is anterior or transverse, and it is transversely directed. Metaloph is transverse, anterior or points backwards.

M3: The labial anteroloph is connected to the paracone or it is of medium length. The lingual anteroloph is always absent. The protoloph is anterior or transverse, and it is transversely directed except in one tooth where it is anterior. The metaloph is transverse, anterior or points backwards. The morphology of the teeth is straight as in the M2.

d4: Normally, protoconid and metaconid are large. When the metalophid I is present, it is connected to the protoconid. The mesolophid is always long and connected to the metaconid, except in one specimen in which it is short. The hypoconulid is always present. The hypolophid is connected to the anterior arm of the hypoconid, and in one tooth it is double (connected to the anterior arm of the hypoconid and to the hypoconulid).

p4: The anterior sinusoid is always triangular. The hypoconid is present or absent. The hypolophid is always present. One tooth bears a hypoconulid.

m1: In all specimens the metalophid I is well connected to the protoconid, and the mesolophid is connected to the metaconid. The hypoconulid is always present. The hypolophid is normally connected to the anterior arm of the hypoconid, but in two specimens it is double, and in the remaining two specimens it is disconnected.

m2: The metalophid I is well connected to the protoconid in all specimens. The mesolophid is always connected to the metaconid, and the hypoconulid is always present. The hypolophid is always connected to the anterior arm of the hypoconid.

m3: The metalophid I is well connected to the protoconid. In all the specimens the mesolophid is long and connected to the metaconid. The hypoconulid is always present. In all specimens the hypolophid is connected to the anterior arm of the hypoconid.

Remarks: The dental characters agree with the diagnosis of *Tataromys sigmodon* MATTHEW & GRANGER, 1923 from the type material of Mongolia (Hsanda Gol Fm., Loh in Mongolia; AMNH 19079, 87570) and with *T. sigmodon* from Ulanatal (China) (WANG 1997: pp. 18–22, figs 12–14; VIANEY-LIAUD *et al.* 2006). The tooth size of the Shine Us species is within the upper size range of *T. sigmodon* given by VIANEY-LIAUD *et al.* (2006). However, the specimens from the Valley of Lakes assemblages (SCHMIDT-KITTLER *et al.* 2006: pp. 182–183, fig. 17; DAXNER-HÖCK *et al.* 2017: p. 174, fig. 44/k–s) are considerably smaller than the specimens from SHU-A/1.

Comparisons of the presently studied *Tataromys sigmodon* from Shine Us and the large-sized *Tataromy plicidens* MATHEW & GRANGER, 1923 show that *T. sigmodon* differs from *T. plicidens* not only by smaller tooth sizes, but also by the more crescentic lophs of the upper and lower teeth. For these comparisons we consider descriptions, figures and measurements of the type material of *T. plicidens* from the Hsanda Gol Fm., in Mongolia coll. AMNH 19082, 28622 a.s.o. (WANG 1997: pp. 10–18, figs 4–11), further materials of *T. plicidens* from Ulan Tatal in China (VIANEY-LIAUD *et al.* 2006), and a few specimens of *T. plicidens* from the Tatal Gol and Hsanda Gol localities in Mongolia figured

by DAXNER-HÖCK *et al.* (2017: p. 174, fig. 44/t–zz). *Tataromys sigmodon* ranges from the lower to the upper Oligocene (letter zone B to C1) in the Valley of Lakes, and is most abundant in letter zone C.

***Tataromys minor* (HUANG, 1985)**

(Fig. 8 B1–B8, Tab. 4)

1985 *Leptotataromys minor* sp. nov. – HUANG: 36–38, fig. 4.

1997 *Tataromys minor* (HUANG, 1958) – WANG: 22–26, figs 15–17, tabs 6–7.

2006 *Tataromys minor* (HUANG, 1958) – VIANEY-LIAUD *et al.*: 132–136, figs 6, 9–10, tabs 12–13, pl. 4.

2017 *Tataromys minor* (HUANG, 1958) – OLIVER *et al.*: 56.

Material: 141 specimens; 5 D4 left (NHMW 2017/0019/0001–0005), 7 D4 right (NHMW 2017/0019/0006–0012), 2 P4 left (NHMW 2017/0019/0013–0014), 4 P4 right (NHMW 2017/0019/0015–0018), 13 M1 left (NHMW 2017/0019/0019–0031), 8 M1 right (NHMW 2017/0019/0032–0039), 10 M2 left (NHMW 2017/0019/0041–0050), 5 M2 right (NHMW 2017/0019/0051–0055), 10 M3 left (NHMW 2017/0019/0056–0065), 1 M3 right (NHMW 2017/0019/0066), 1 fragmentary maxilla with M1–2 right (NHMW 2017/0019/0040), 5 d4 left (NHMW 2017/0019/0067–0070, 2017/0019/0092), 5 d4 right (NHMW 2017/0019/0071–0074, 2017/0019/0141), 6 p4 left (NHMW 2017/0019/0075–0080), 4 p4 right (NHMW 2017/0019/0081–0084), 7 m1 left (NHMW 2017/0019/0085–0091), 13 m1 right (NHMW 2017/0019/0093–0105), 10 m2 left (NHMW 2017/0019/0107–0116), 10 m2 right (NHMW 2017/0019/0117–0126), 9 m3 left (NHMW 2017/0019/0127–0135), 5 m3 right (NHMW 2017/0019/0136–0140), 1 fragmentary mandible with m1–2 right (NHMW 2017/0019/0106).

Table 4. Descriptive statistics of *Tataromys minor* from Shine Us. n = number of teeth measured.

	length (mm)			width (mm)	
	range	mean	n	range	mean
D4	1.08–1.25	1.16	5/7	0.59–1.21	1.01
P4	0.85–0.98	0.93	4/4	1.09–1.26	1.17
M1	1.14–1.45	1.34	16/20	1.11–1.42	1.26
M2	1.43–1.60	1.51	10/10	1.37–1.50	1.44
M3	1.38–1.66	1.48	9/8	1.33–1.47	1.41
d4	1.16–1.28	1.23	3/7	0.80–0.84	0.81
p4	1.00–1.20	1.07	8/10	0.69–0.94	0.81
m1	1.14–1.59	1.45	10/14	0.99–1.18	1.09
m2	1.47–1.80	1.59	17/19	1.08–1.33	1.17
m3	1.61–1.82	1.69	10/10	1.09–1.40	1.23

Measurements: see Tab. 4.

Description: D4: The labial anteroloph is always present. The lingual anteroloph is absent. Half of the specimens have a hypoconid and hypolophid.

P4: The labial anteroloph is incipient or absent. The lingual anteroloph is absent. The labial posteroloph is medium-sized or absent. The lingual posteroloph is absent except in one specimen in which it is incipient.

M1: The labial anteroloph is present in all specimens. The lingual anteroloph is absent. The protoloph is always anterior, and it is transversely directed or it is slightly retroverse. The metaloph points backwards: it is transverse, anterior or disconnected. The metaloph is retroversely directed or transverse.

M2: The labial anteroloph is long or medium, and in one tooth short. The lingual anteroloph is absent. The protoloph is anterior except in one specimen it is transverse. The metaloph points backwards, it is transverse, anterior or disconnected. The orientation of the metaloph is very variable; it is retroverse, transverse or even proverse.

M3: The labial anteroloph is medium or short. The lingual anteroloph is absent. The protoloph is anterior, transverse or double. The metaloph is retroversely directed, transverse or proverse. The morphology of the teeth is swollen and bulky, or straight as in M2.

d4: The metalophid I is absent or it is present and connected to the protoconid. The mesolophid is absent or it is long and connected to the metaconid. The hypoconulid is always present. The hypolophid is disconnected; it is directly connected to the hypoconid or it is connected to the anterior arm of the hypoconid. In three specimens the protoconid and metaconid are very well developed.

m1: The metalophid I is well connected to the protoconid in all specimens. The mesolophid is always connected to the metaconid, except in one tooth in which it is of medium length. The hypoconulid is short. The hypolophid is always connected to the anterior arm of the hypoconid.

m2: The metalophid I is well connected to the protoconid, except in one specimen in which it is absent. The mesolophid is connected to the metaconid, except in two teeth in which it is absent. The hypoconulid is always present. In all specimens the hypolophid is connected to the anterior arm of hypoconid.

m3: The metalophid I is always present. The mesolophid is long and connected to the metaconid except in one tooth. In all specimens the hypoconulid is present and the hypolophid is connected to the anterior arm of the hypoconid.

Remarks: This species is the smallest of all Ctenodactylidae from the Shine Us assemblage. The teeth are brachyodont and of buno-lophodont pattern. Both, the dental characters and size agree with *Tataromys minor* from Ulantatal (VIANEY-LIAUD *et al.* 2006). The Shine Us specimens differ from *Tataromys minor longidens* from the Valley of Lakes (Mongolia) by the less elongated upper molars. For comparisons see SCHMIDT-KITTLER *et al.* (2006: pp. 183–187, fig. 21, pl. 1, figs A–F). The stratigraphic

range of *T. minor longidens* from the Valley of Lakes localities is lower to upper Oligocene (letter zone C to C1), with the highest abundances in letter zone C.

Genus *Yindirtemys* BOHLIN, 1946

***Yindirtemys cf. ulantatalensis* (HUANG, 1985)**

(Fig. 8 C1–C2)

1985 *Tataromys ulantatalensis* sp. nov. – HUANG: 28–29, fig. 1, pl. 1, figs 1–3.

1997 *Buonomys ulantatalensis* (HUANG, 1985) – WANG: 45–48, fig. 29, tabs 18–19.

2006 *Yindirtemys ulantatalensis* (HUANG, 1985) – VIANEY-LIAUD *et al.*: 146–153, figs 14–16, tabs 20–21, pls 8–10.

Material and measurements: ten specimens; fragmentary right m1–2 (NHMW 2017/0020/0001), width = 1.81 mm; right m2 (NHMW 2017/0020/0002), length = 2.35 mm, width = 1.87 mm; fragmentary left m1–2 (NHMW 2017/0020/0003); fragmentary left m1–2 (NHMW 2017/0020/0004), width = 1.92 mm; fragmentary left m3 (NHMW 2017/0020/0005), length = 2.67 mm, width = 1.97 mm; fragmentary left m3 (NHMW 2017/0020/0006), width = 2.23 mm; fragmentary right m3 (NHMW 2017/0020/0007), width = 1.81 mm; fragmentary left M3 (NHMW 2017/0020/0008), width = 2.64 mm; fragmentary left M2–3 (NHMW 2017/0020/0009); fragmentary left M1–2 (NHMW 2017/0020/0010), width = 2.59 mm.

Description: M1–2: In the only specimen, the labial and the posterior part of the tooth are broken. The labial anteroloph is of medium length. The lingual anteroloph is absent.

M2–3: The tooth has a broken anterior and lingual part. The proto-loph is transverse and transversely directed. The metaloph is transverse and retroversely directed.

M3: The anterior part of the specimen is broken. The metaloph is transverse and retroversely directed.

m1–2: The mesolophid is connected to the metaconid. The hypoconulid is always present. The hypolophid is connected to the anterior arm of the hypoconid.

m2: Only one tooth is available. The metalophid I is connected to the protoconid. The mesolophid is connected to the metaconid. The hypoconulid is always present. The hypolophid is connected to the anterior arm of the hypoconid.

m3: The mesolophid is long and connected to the metaconid. The hypoconulid is present. The hypolophid is double (connected to the anterior arm of the hypoconid and connected to the mesolophid) or it is connected to the anterior arm of the hypoconid.

Remarks: This *Yindirtemys* form is medium sized, brachyodont and bunolo-phodont.

The material is very scarce and most of the teeth are fragmentary. The dental characters of the Shine Us specimens agree with the original diagnosis of *Yindirtemys ulantatalensis* (HUANG 1985). The size ranges, however, are in the lower size variation of the type material from Ulantatal.

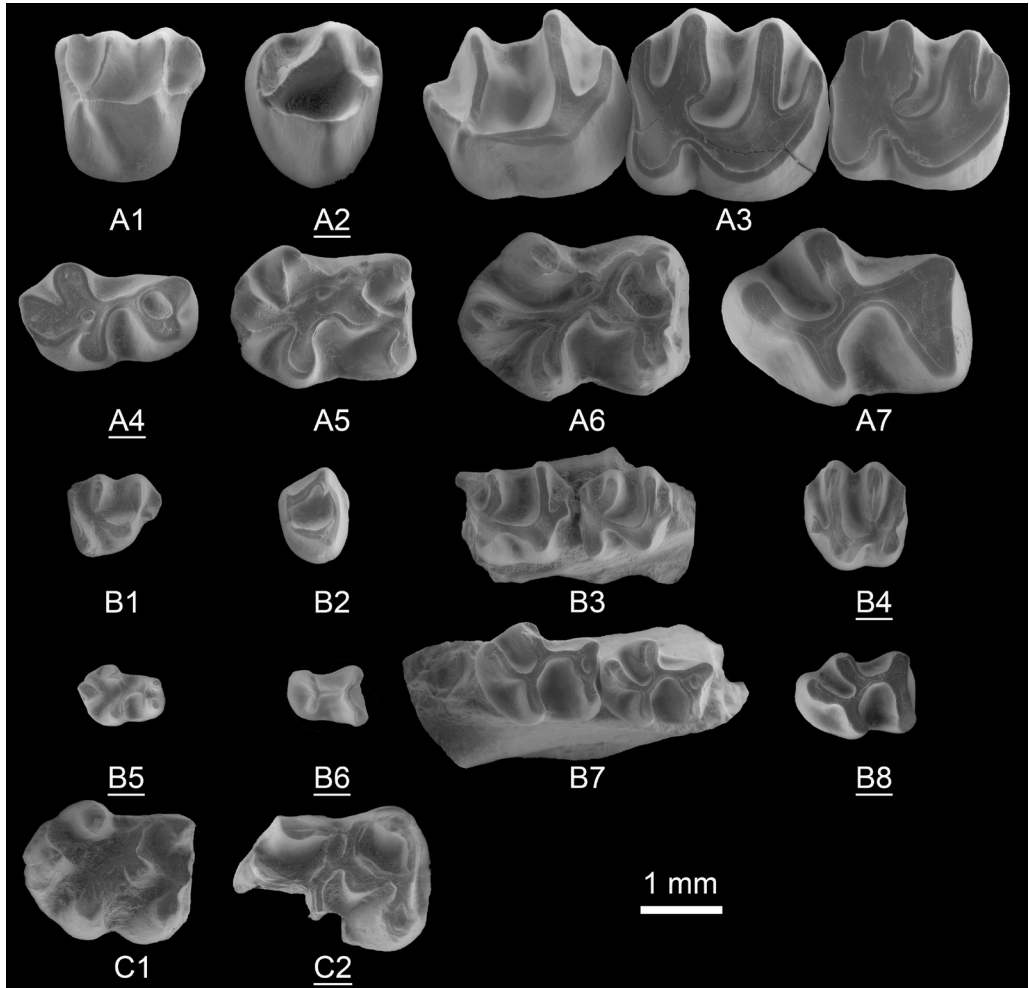


Fig. 8. Ctenodactylidae from the Shine Us locality (assemblage SHU-A/1), Khaliun Basin, south western Mongolia, Beger Fm., upper Oligocene. *Tataromys sigmodon*: **A1**: D4 right (NHMW 2017/0018/0017), **A2**: P4 left (NHMW 2017/0018/0025), **A3**: M1–M3 right (NHMW 2017/0018/0048), **A4**: d4 left (NHMW 2017/0018/0071), **A5**: m1 right (NHMW 2017/0018/0105), **A6**: m2 right (NHMW 2017/0018/0116), **A7**: m3 right (NHMW 2017/0018/0121). *Tataromys minor*: **B1**: D4 right (NHMW 2017/0019/0006), **B2**: P4 right (NHMW 2017/0019/0015), **B3**: M1–M2 right (NHMW 2017/0019/0040), **B4**: M3 left (NHMW 2017/0019/0062), **B5**: d4 left (NHMW 2017/0019/0068), **B6**: p4 left (NHMW 2017/0019/0078), **B7**: m1–m2 right (NHMW 2017/0019/0106), **B8**: m3 left (NHMW 2017/0019/0131). *Yindirtemys cf. ulantatalensis*: **C1**: m2 right (NHMW 2017/0020/0002), **C2**: m2–3 left (NHMW 2017/0020/0005). Scale bar 1 mm. All left side specimens are inverted and the numbers are underlined.

Cricetidae (P. LÓPEZ-GUERRERO)

For dental terminology see MARIDET *et al.* (2009: fig.1).

Family Cricetidae FISCHER VON WALDHEIM, 1817

Genus *Witenia* DE BRUIJN, ÜNAY, SARAÇ & YILMAZ, 2003

***Witenia* sp.**

(Fig. 9 A)

2003 *Witenia* n. gen. – DE BRUIJN, ÜNAY, SARAÇ & YILMAZ: 69–71.

2017b *Witenia* sp. – LÓPEZ-GUERRERO, MARIDET & DAXNER-HÖCK: 106, fig. 4j.

Material: 1 specimen; 1 right m3 (NHMW 2018/0136/0001). length = 2.23 mm; width = 1.79 mm.

Description: Large-sized bunodont molar with both lingual and labial anterolophids well developed. The metalophulid I is present and connected to the anterolophulid. The metalophulid II is absent. The ectolophid bears a large mesolophid that reaches the lingual edge of the molar. The ectomesolophid is very weak. The entoconid is well developed and the hypoconid hind arm is present but short. The anteriorly directed hypolophulid is connected to the entolophid.

Remarks: The large size of the specimen precludes assignment to the genus *Eucricetodon*, which occurs frequently in Valley of Lakes localities (LÓPEZ-GUERRERO *et al.* 2017a). Its size is similar to the genera *Edirnella* and *Witenia*. *Edirnella* possess a well-developed mesolophulid that connects to the entoconid (DE BRUIJN *et al.* 2003), which is not present in the Shine Us specimen. Our molar shares a number of traits with *Witenia* such as: the equal development of the anterolophids, the anteriorly directed hypolophulid and the long mesolophid. The tooth size of the presently studied specimen is similar to that of *Witenia fusca* from the Eo/Oligocene locality of Shüngülü (DE BRUIJN *et al.* 2003) and *Witenia yolua* from the upper Oligocene of Ulantatal in China (GOMES RODRIGUES *et al.* 2012a). With regard to the scarcity of the material we name the Shine Us specimen *Witenia* sp.

Genus *Eucricetodon* THALER, 1966

***Eucricetodon asiaticus* (MATTHEW & GRANGER, 1923)**

(Fig. 9 B1–B2)

1923 *Eumys asiaticus* new species – MATTHEW & GRANGER: 7, fig. 9.

1978 *Eucricetodon asiaticus* – LINDSAY: 590–595.

2017a *Eucricetodon asiaticus* – LÓPEZ-GUERRERO, MARIDET & DAXNER-HÖCK: 68, fig. 3.

Material: 4 specimens; 1 right fragmented M1 (NHMW 2018/0139/0001), width = 1.74 mm; 1 lingual fragment of an M1 (NHMW 2018/0139/0002); 1 right m1 (NHMW 2018/0139/0003), length = 2.15 mm, width = 1.28 mm; 1 fragmentary lower molar (NHMW 2018/0139/0004).

Main characteristics of the genus: The studied material shows several characters that lead us to assign it to *Eucricetodon*: the presence of a simple anterocone, the anterior arm of the protocone is free and the anteroloph is connected to the protocone of M1. Also, the anteroconid of m1 is placed on the longitudinal axis of the teeth and the posterior arm of the protoconid ends freely on m2 (LÓPEZ-GUERRERO *et al.* 2017a).

Description: M1: One of the specimens is a fragment of the lingual part, so we describe in detail the other specimen which is also incomplete anterolabially. Its crown is high: the cusps are stout and rounded. The anterior part is missing. An anterocone spur is absent. The paracone is rounded and has a very short spur. The mesosinus is open. The mesostyle is absent. The mesoloph is short. The metalophule is connected transversally to the hypocone. The sinus is directed forward. The posteroloph is long and reaches the metacone. There is no lingual cingulum.

m1: This molar has an elongated shape. The anteroconid is situated on the longitudinal axis of the tooth. It is transversally elongated. The labial anterolophid is a well-developed ridge that connects anteroconid with a weak protoconid. The lingual anterolophid is present but weak and a small cusp can be observed. The anterolophulid is not present. The metalophulid I is missing and the metalophulid II is connected to the posterior arm of the protoconid. The ectolophid bears a very weak mesolophid. The ectomesolophid is incipient. The entoconid spur is present but weak. The hypoconid hind arm is absent. The hypolophulid is short and connected to the ectolophid. The sinusid is short and wide, transversally directed.

Remarks: The size of the studied material is similar to *Aralocricetodon schokensis* from the Valley of Lakes (LÓPEZ-GUERRERO *et al.* 2017b). The M1, however, has a transversal metalophule whereas *A. schokensis* displays it posteriorly. Also, *A. schokensis* has no posterior spur of the paracone and the m1 possess a strong metalophulid I connected to the anteroconid, which is labially displaced. On the other hand, in addition to the size, the material from Shine Us presents a number of features that fit the emended diagnosis of *Eucricetodon asiaticus* proposed by GOMES RODRIGUES *et al.* (2012a) such as: bunodont teeth; the M1 with a simple anterocone and an anterior arm of the protocone usually free; a metalophule joining the mesial or middle part of the hypocone. The m1 have a simple anteroconid linked to the protoconid.

***Eucricetodon jilantaiensis* GOMES RODRIGUES, MARIVAUX & VIANEY-LIAUD, 2012A**
(Fig. 9 C1–C7, Tab. 5)

2012a *Eucricetodon jilantaiensis* nov. sp. – GOMES RODRIGUES, MARIVAUX & VIANEY-LIAUD: 166, fig. 4.

2017a *Eucricetodon jilantaiensis* – LÓPEZ-GUERRERO, MARIDET & DAXNER-HÖCK: 83, fig. 6.

Material: 47 specimens; 8 M1 (NHMW 2018/0137/0001–0008); 7 M2 (NHMW 2018/0137/0009–0015); 6 M3 (NHMW 2018/0137/0016–0021); 4 m1 (NHMW 2018/0137/0022–0023, 2018/0137/0025–0026); 1 m1–m2 (NHMW 2018/0137/0024); 10 m2 (NHMW 2018/0137/0026–0035); 12 m3 (NHMW 2018/0137/0036–0047).

Measurements: see Tab. 5.

Description: M1: A prelobe is not present. An anterocingulum is absent. The anterocone is large, is labially displaced and not split. The labial anteroloph is always present. The anterocone spur is always present and starts from the labial part of anterocone; it is long and ends freely on the anterosinus or it is labially curved. In one specimen it is connected to the paracone. The anterolophule is present and connects the anterior arm of the protocone with the lingual part of the anterocone. There is no platform on the protosinus. The paracone has a weak spur. The protolophule II is present and connected to the entoloph. The mesoloph is always present and short. The metalophule is connected to the posteroloph. The posteroloph is long and reaches the metacone. The sinus is directed forward.

M2: Both lingual and labial anterolophs are well developed. The anterolophule is thick and bears a small ridge in one molar. The protolophule II is present and connected to the entoloph. The protolophule spur is absent. The protocone lacks a posterior arm; it is connected to the entoloph only through the anterior arm. The entoloph bears a long mesoloph that never reaches the labial border. The second mesoloph is absent. The paracone spur is always present and long in some cases. The entomesoloph is present in a few specimens. The metalophule is connected to the middle part of the hypocone or it is joined to the posterior arm of the hypocone. The sinus is directed forward.

M3: The labial anteroloph is present and long, and the lingual anteroloph is absent. The protolophule I is present and connected to the anterolophule. The protolophule II is absent. A paracone spur is absent. The entoloph is incomplete in some cases and it is connected neither to the protolophule nor to the metalophule. The mesoloph is short. The

Table 5. Descriptive statistics of tooth measurements of *Eucricetodon jilantaiensis* from assemblage SHU-A/1, locality Shine Us, Khaliun Basin, south western Mongolia.

	length (mm)			width (mm)	
	range	mean	n	range	mean
M1	1.99–2.24	2.08	5/5	1.29–1.43	1.34
M2	1.70–1.81	1.76	5/3	1.40–1.54	1.48
M3	1.15–1.36	1.22	5/4	1.10–1.21	1.15
m1	1.98–2.07	2.02	2/2	1.21–1.33	1.27
m2	1.78–1.98	1.92	4/7	1.21–1.49	1.41
m3	1.58–1.80	1.66	7/7	1.22–1.36	1.29

neontoloph is present and joins the protocone with the hypocone. The sinus is narrow and short. The hypocone is very much reduced. The posteroloph is always present and long. The mesosinus is closed by a cingulum.

m1: The anteroconid is large and situated on the longitudinal axis of the occlusal surface; it is rounded. The labial anterolophid is present but thin and short. The lingual anterolophid is absent in some specimens (Fig. 9 C4) or very weak (Fig. 9 C7). The anterolophulid is absent. The metalophulid I is present and joined to lingual part of the anterocone. The metalophulid II is present and connected to the posterior arm of the protoconid. The mesolophid is incipient, short or absent. The ectolophid is enlarged in its middle section as a mesoconid. The ectomesolophid is usually present, frequently short or incipient. The hypoconid hind arm is absent. The hypolophulid is short and connected to the ectolophid.

m2: Both labial and lingual anterolophids are present and well developed. The metalophulid I is present and connected to the anterolophulid. The metalophulid II is absent. The posterior arm of the protoconid is well-developed and ends freely in the mesosinusid. The mesolophid is absent or very weak. In most teeth the ectomesolophid is present, but it is short or incipient. The ectolophid is oblique. The hypolophulid is connected where the ectolophid and the anterior arm of the hypoconid are joined. The hypoconid hind arm is absent.

m3: The labial anterolophid is short but reaches the protoconid. The lingual anterolophid is also short and connected to the metaconid. The metalophulid I is present and connected to the lingual anterolophid. The metalophulid II and the metalophulid spur are absent. The ectolophid is long and thin. The mesolophid is long and reaches the labial border. The ectomesolophid is always absent. The entoconid is reduced and small. The hypolophulid is attached to the anterior part of the hypoconid. The hypoconid hind arm is absent.

Remarks: The studied fossils present features that agree with the diagnosis of *Eucricetodon* such as the simple anteroconid, the anteroconespur and the lingual anteroloph connected to the protocone on M1. It also lacks the anterolophulid on m1, and the posterior arm of the protoconid ends freely on m2. The material is similar in size to *Eucricetodon caducus* and *Eucricetodon jilantaiensis*. However, *E. caducus* presents an elongated anterocone without anterocone spur and transversal metalophule on M1; anterolophulid and wider sinusids on m1; and short mesolophid on m3 (LÓPEZ-GUERRERO *et al.* 2017a). Contrarily, the specimens share several characteristics with *E. jilantaiensis* from the nearby localities in the Valley of Lakes. M1 presents an anterocone spur that ends freely in the anterosinus, a short paracone spur, a small anteroloph that is linked to the protocone and a posterior metalophule. M2 has also a posteriorly directed metalophule and a paracone spur that can be connected to the mesoloph. The anterolophulid of m1 is missing and the sinusid is narrow; it also has both metalophulids I and II.

***Eucricetodon bagus* GOMES RODRIGUES, MARIVAUX & VIANEY-LIAUD, 2012a**
(Fig. 9 D1–D9, Tab. 6)

2012a *Eucricetodon bagus* nov. sp. – GOMES RODRIGUES, MARIVAUX & VIANEY-LIAUD: 167, fig. 5.
2017a *Eucricetodon bagus* – LÓPEZ-GUERRERO, MARIDET & DAXNER-HÖCK: 80, fig. 5.

Material: 54 specimens; 5 M1 (NHMW 2018/0138/0001–0005), 9 M2 (NHMW 2018/0138/0006–0014), 7 M3 (NHMW 2018/0138/0015–0021), 9 m1 (NHMW 2018/0138/0023–0031), 1 mand m1–m2 (NHMW 2018/0138/0032), 20 m2 (NHMW 2018/0138/0022, 2018/0138/0033–0048, 2018/0138/0055–0057); 3 m3 (NHMW 2018/0138/0049–0051).

Measurements: see Tab. 6.

Description: M1: The anterocone is elongated and usually simple, but can be slightly split. A labial anteroloph is present; it covers the anterosinus and it is fused with the paracone. The lingual anteroloph is well developed and originates from the apex of the anterocone and joins the protocone. The anterocone spur is always present; it is long and connected to the protocone spur or ends freely in the anterosinus. The anterolophule is present and connected to the lingual part of the anterocone. The protolophule I is missing. The posterior spur of the paracone is always present, but is very weak and short. All teeth have a short mesoloph. The metalophule is posteriorly directed and is connected to the posterior arm of the hypocone or to the posteroloph.

M2: Both lingual and labial anterolophs are well developed. The protolophule I is present and connected to the point where the anterolophule is joined to the anterior arm of the protocone or it ends freely in the anterosinus. The protolophule II is present. The entoloph is straight and long; it bears a well developed mesoloph that never reaches the labial border. The paracone spur is always present. The entomesoloph is absent. The metalophule is connected to the entoloph, clearly anterior to the hypocone in some cases.

M3: The labial anteroloph is present and long, and the lingual anteroloph is absent. The protolophule I is present and connected to the short anterolophule. The protolophule II

Table 6. Descriptive statistics of tooth measurements of *Eucricetodon bagus* from assemblage SHU-A/1, locality Shine Us, Khaliun Basin, south western Mongolia.

	length (mm)			width (mm)	
	range	mean	n	range	mean
M1	1.74–1.81	1.79	4/3	1.24–1.29	1.26
M2	1.32–1.60	1.48	8/8	1.12–1.38	1.27
M3	0.99–1.08	1.03	3/3	1.02–1.11	1.07
m1	1.44–1.71	1.55	5/8	0.96–1.13	1.03
m2	1.48–1.65	1.54	14/14	1.09–1.27	1.19
m3	1.22–1.39	1.33	3/3	1.09–1.16	1.14

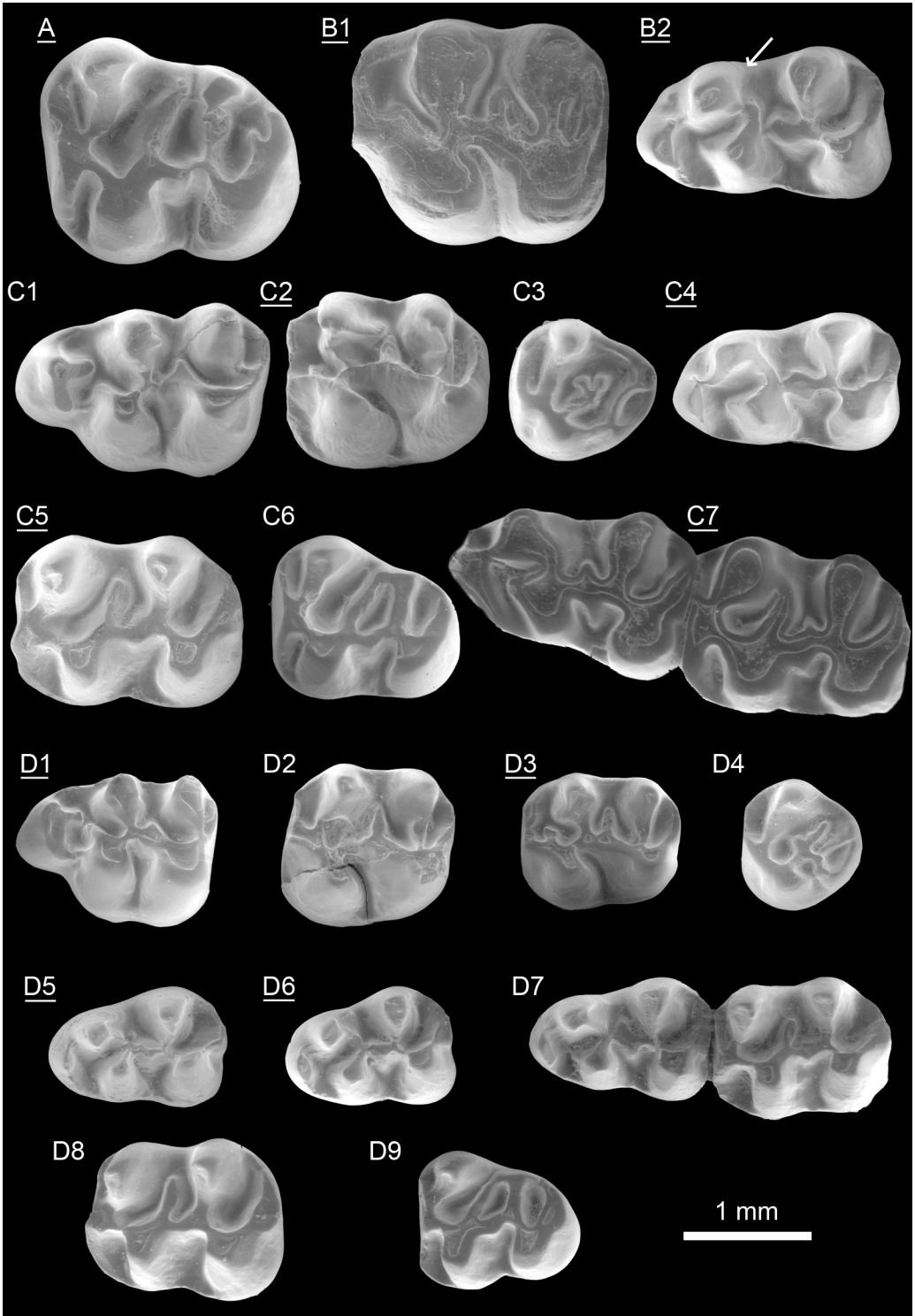
is absent. Some molars have a small paracone spur. The anterior part of the entoloph is incomplete. The posterior arm of the protocone is connected to the mesoloph, which is long but never reaches the labial border. The posterior part of the entoloph is present and joined to the metalophule. The neoentoloph can be present or absent. The metalophule is connected to the point where the anterior arm of the hypocone and the entoloph are connected. The posteroloph is always present and long.

m1: This molar is elongated. The anteroconid is situated on the longitudinal axis of the occlusal surface; it is transversally elongated and simple. The labial anterolophid is a well-developed ridge that connects the anteroconid with the labial part of the protoconid. The lingual anterolophid is missing or very short. The anterolophulid is present in some molars and connected to the labial part of the anteroconid; it can be absent or join the metaconid instead of the protoconid. The metalophulid I is present in some specimens. The metalophulid II is present and connected to the posterior arm of the protoconid. The ectolophid is joined to the posterior arm of the protoconid. The mesolophid is weak or absent. The ectomesolophid is always present and is weak but distinguishable. The hypoconid hind arm is always absent.

m2: Both labial and lingual anterolophids are present. The metalophulid I is present and it is connected to the point where the labial anterolophid and the anterolophulid are joined. The metalophulid II is always absent. The posterior arm of the protoconid is connected to the ectolophid. It ends freely in one specimen. The mesolophid is always present, long, but does not reach the lingual border. The ectomesolophid is absent. The ectolophid is straight. The hypolophulid is transverse and connected to the posterior part of the ectolophid. The hypoconid hind arm is absent. The posterolophid is long and displays a constriction.

m3: The labial anterolophid is long and reaches the protoconid. The lingual anterolophid is shorter and does not reach the metaconid. The metalophulid I is present and connected to the lingual anterolophid. The metalophulid II is always absent. The metalophulid spur is present in one specimen and it starts from the metalophulid I. The ectolophid bears a long mesolophid that can reach the lingual border or it is curved and attached to the entoconid. The small entoconid is reduced, the hypoconid hind arm is absent, and the transverse hypolophulid is connected to the entolophid.

Remarks: The studied material shows several characters that lead us to assign it to *Eucricetodon* such as: the presence of a simple anterocone, the anterior arm of the protocone free and the anteroloph connected to the protocone on M1. Also, the anteroconid on m1 is placed on the longitudinal axis of the teeth and the posterior arm of the protoconid ends freely on m2 (LÓPEZ-GUERRERO *et al.* 2017a). The morphology and size of the Shine Us material fit with the diagnosis of *Eucricetodon bagus* described from Ulan-tatal by GOMES RODRIGUES *et al.* (2012a). M1 has a simple anterocone and frequently a double connection between the anterocone and a protocone via the anterolophule and the anterior arm of the protocone. In comparison with the specimens of *E. bagus* from the Valley of Lakes (LÓPEZ-GUERRERO *et al.* 2017a) the material from Shine Us presents



slight differences in the lengths of M2, m1 and m2. However, it shares a number of morphological traits including the metalophule connected to the posterior part of the hypocone or to the posteroloph on M1. The protolophule I and II are present on M2, which bears a weak paracone spur. The anterior part of the entoloph on M3 is missing and some m1 exhibits a mesoconid and both metalophulids I and II.

Dipodidae (G. DAXNER-HÖCK)

For dental terminology see DAXNER-HÖCK *et al.* (2014: fig. 3).

Family Dipodidae FISCHER VON WALDHEIM, 1817

Genus *Heosminthus* WANG, 1985

Heosminthus chimidae DAXNER-HÖCK, BADAMGARAV & MARIDET, 2014

(Fig. 10 A1–A8, Tab. 7)

2014 *Heosminthus chimidae* nov. spec. – DAXNER-HÖCK, BADAMGARAV & MARIDET: 147–151, fig. 7/1–18, tab. 5.

Material: 127 specimens; 1 P4–M2 left (NHMW 2018/0029/0011), 16 M1 left (NHMW 2018/0029/0001–0010, 2018/0029/0012–0016, 2018/0029/0024), 7 M1 right (NHMW 2018/0029/0017–0023), 1 P4–M1 right (NHMW 2018/0029/0025), 10 M2 left (NHMW 2018/0029/0026–0035), 7 M2 right (NHMW 2018/0029/0036–0042), 5 M3 left (NHMW 2018/0029/0043–0047), 5 M3 right (NHMW 2018/0029/0048–0052), 18 m1 left (NHMW 2018/0029/0053–0070), 1 m1–3 left (NHMW 2018/0029/0071), 22 m1 right (NHMW 2018/0029/0072–0083), 15 m2 left (NHMW 2018/0029/0084–0098), 8 m2 right (NHMW 2018/0029/0099–0106), 4 m3 left (NHMW 2018/0029/0107–0110), 7 m3 right (NHMW 2018/0029/0110–0116), 11 P4 (NHMW 2018/0029/0121–0130, 2018/0029/0117).

- ◀ Fig. 9. Cricetidae from the Shine Us locality (assemblage SHU-A/1), Khaliun Basin, south western Mongolia, Beger Fm., upper Oligocene. *Witenia* sp.: **A**: right m3 (NHMW 2018/0136/0001). *Eucricetodon asiaticus*: **B1**: right M1 (NHMW 2018/0139/0001), **B2**: right m1 (NHMW 2018/0139/0003). *Eucricetodon jilantaiensis*: **C1**: left M1 (2018/0137/0004), **C2**: right M2 (NHMW 2018/0137/0009), **C3**: left M3 (NHMW 2018/0137/0019), **C4**: right m1 (NHMW 2018/0137/0025), **C5**: right m2 (NHMW 2018/0137/0034), **C6**: left m3 (NHMW 2018/0137/0039), **C7**: right m1–m2 (NHMW 2018/0137/0024). *Eucricetodon bagus*: **D1**: right M1 (NHMW 2018/0138/0003), **D2**: left M2 (NHMW 2018/0138/0009), **D3**: right M2 (NHMW 2018/0138/0011), **D4**: left M3 (NHMW 2018/0138/0019), **D5**: right m1 (NHMW 2018/0138/0023), **D6**: right m1 (NHMW 2018/0138/0030), **D7**: left m1–m2 (NHMW 2018/0138/0032), **D8**: left m2 (NHMW 2018/0138/0033), **D9**: left m3 (NHMW 2018/0138/0049). All right side specimens are inverted and the numbers underlined.

Measurements: see Tab. 7.

Main characteristics of the genus (DAXNER-HÖCK *et al.* 2014: p. 142): Upper and lower molars are of small to medium size, bunodont and low crowned. The upper molars M1–2 are almost square in occlusal outline, have a concave occlusal surface, two pairs of cusps in opposite position, and three roots (one wide lingual, two rounded labial). Contrarily to *Plesiosminthus* which has grooved upper incisors (SCHAUB 1930: p. 618), the upper incisor of *Heosminthus* has a smooth anterior surface.

Description: P4: One cusp is surrounded by a posterior cingulum.

M1–2: The M1–2's are rapezoidal to almost square in occlusal outline and have rounded corners. Labially the teeth are wider than lingually. They have four rounded cones in opposite position. The cones are higher than the lophes. The mesoloph and the posteroloph are long, reaching the labial margin of the tooth. The protoloph, metaloph and entoloph are short. The metaloph is connected with the hypocone. No posterior sulcus is present. The sinus is wide and shallow, symmetrical or directed forward. The M1–2's have three roots. The lingual root is flat, antero-posteriorly enlarged, in a few specimens the tip is split. The labial roots are rounded.

M1: It has a long anterior arm of the protocone and a protoloph II. Additionally, two M1 show an anterior labial cingulum, and one M1 has protoloph I+II.

M2: It has a long labial cingulum; the lingual one is weak or absent. The protoloph is single or double. The protoloph I is always present, the protoloph II is either continuous (50%), constricted or weak, or absent.

M3: It is the smallest upper molar. The sinus is closed, the lophes vary in length and number. The M3 has three roots.

The lower molars are longer than wide, have four main conids, and four distinct lophids. The conids are higher than the lophids. The lower molars have two roots.

Table 7. Descriptive statistics of tooth measurements of *Heosminthus chimidae* from assemblage SHU-A/1, locality Shine Us, Khaliun Basin, south western Mongolia.

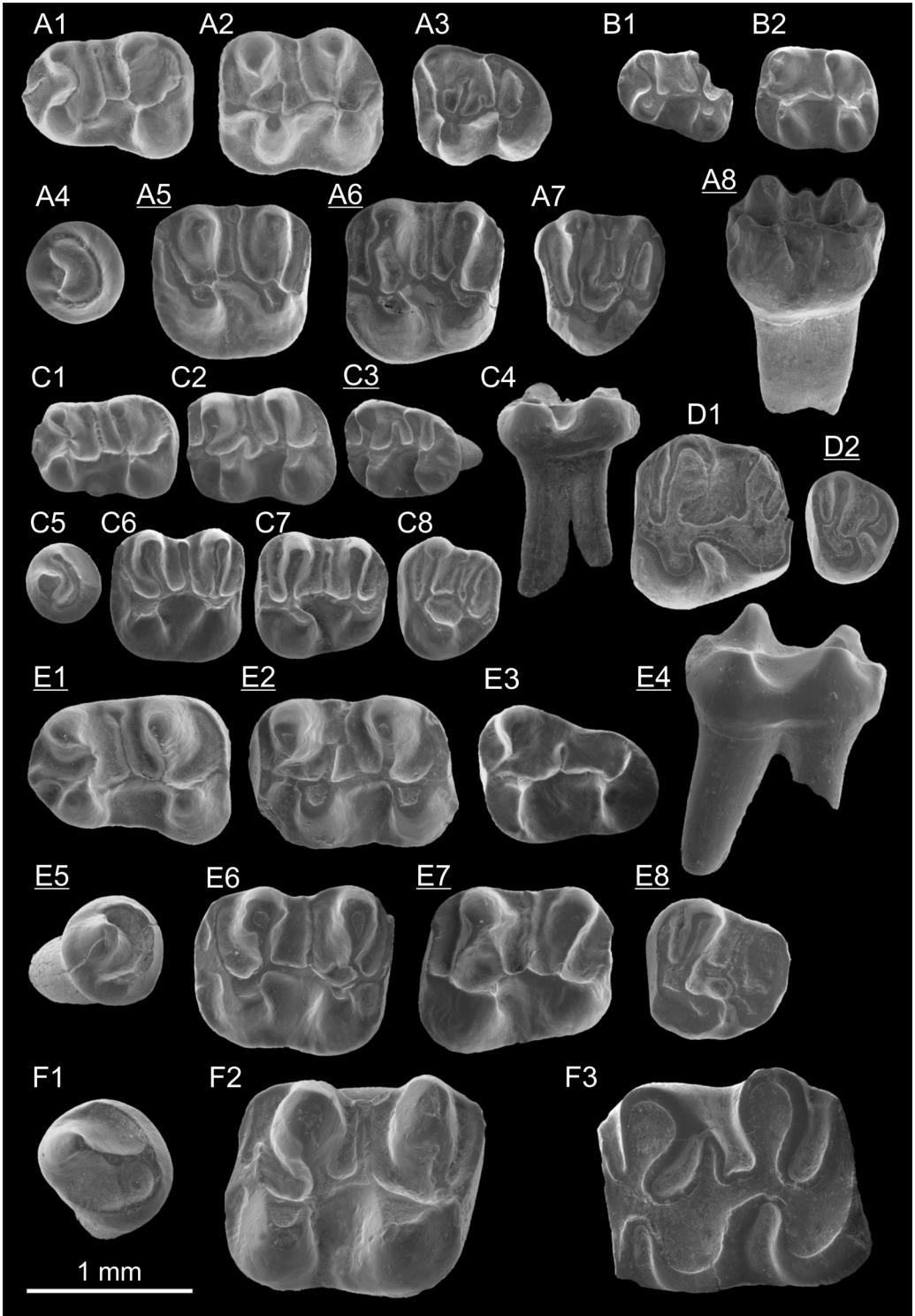
	length (mm)			width (mm)	
	range	mean	n	range	mean
P4	0.56–0.64	0.59	9	0.56–0.64	0.59
M1	0.96–1.22	1.09	22	0.87–1.06	0.99
M2	0.92–1.13	1.01	15/14	0.89–1.06	0.96
M3	0.71–0.87	0.79	9/10	0.78–0.94	0.86
m1	0.96–1.22	1.10	29/28	0.73–0.87	0.81
m2	0.94–1.18	1.06	21	0.75–0.94	0.86
m3	0.82–0.94	0.87	9/11	0.68–0.82	0.74

m1: It is rectangular in occlusal outline, narrowed in the anterior part and widest in the posterior part. 80% of the m1 have an isolated anteroconid, 20% a lingual anterior cingulid attached to the anteroconid. The metalophid exceeds all other lophids in elevation. The low mesolophid is long (100%), ending labially in a mesoconid (90%) and lingually in a mesostylid (45%). The short hypolophid is connected with the anterior arm of the hypoconid or the ectolophid, respectively. The longitudinal or oblique ectolophid attaches to the protoconid or its basal part. The pronounced posterolophid continues to the base of the entoconid, rarely to its top. 90% of m1 have a hypoconulid, and 50% a posterior sinusid. The sinusid is shallow.

m2: It is nearly rectangular in occlusal outline. The lingual and labial anterolophids are more or less equally long and are connected by the anteroconid. Almost 50% of m2 show only the posterior arm of the protoconid, and 50% have both a long mesolophid and a short posterior arm of the protoconid. The mesoconid is usually present, the mesostylid not. The metalophid is connected to the anterior arm of the protoconid, the hypolophid to the anterior arm of the hypoconid. The pronounced posterolophid shows a hypoconulid in 25% of the m2, and a posterior sinusid is also present in 25% of these teeth.

m3: It is similar to m2, but narrowed posteriorly. The main differences from the m2 are: the entoconid is very weak, and the posterior arm of the protoconid dominates over the mesolophid.

Remarks: No grooved upper incisor was found in the fossil collection of SHU-A/1, thus *Plesiosminthus* can be excluded. The dental characteristics of the Shine Us specimens are within the morphological variation of *H. chimidae* from the Valley of Lakes assemblages, and the tooth measurements agree with the lower to medium size range of this species. So far, *H. chimidae* has been documented by > 2,400 fossils from thirty-four fossil beds of the Taatsiin Gol and Taatsiin Tsaagan Nuur region (Valley of Lakes), stratigraphically ranging from the lower Oligocene to the Oligocene–Miocene transition. In the course of these nine million years, *H. chimidae* developed a wide variability of dental morphology and size (DAXNER-HÖCK *et al.* 2014: pp. 147–151, tab. 5, fig. 7). The genus *Heosminthus* includes three more species: *H. primiveris* WANG, 1985, *H. nomogenesis* LI, GONG & WANG, 2017, and *H. borrae* DAXNER-HÖCK, BADAMGARAV & MARIDET, 2014. *H. primiveris* and *H. nomogenesis* are known from the upper Eocene of Caijachong (Yunnan, China) and Erden Obo (Nei Mongol, China), respectively. *H. borrae*, ranging from the lower Oligocene to lower Miocene, was documented from the Taatsiin Gol and Taatsiin Tsaagan Nuur regions (Valley of Lakes, Mongolia). The two Eocene species, *H. primiveris* and *H. neimogenesis*, show more primitive dental characters than the Oligocene species, *e.g.*, the narrow anterior part of M1, the short anterior arm of the protoloph, a distinct anterior cingulum of M1, and the weak lophids of lower molars (WANG 1985: figs 10–11; LI *et al.* 2017). *H. borrae*, however, has the most derived dental characteristics. It differs from *H. chimidae* by smaller size and the following features: the cones/conids tend to become lophodont, the loph/lophids are almost as high as cones/conids, the valleys are narrow and deep, the protoloph II of M2 is weak or



absent, the lingual anterolophid of m2–3 is pronounced, the labial one absent or weak, and the posterior arm of the protoconid (m2–3) is short or absent (DAXNER-HÖCK *et al.* 2014: p. 143, fig. 6, tab. 4; DAXNER-HÖCK *et al.* 2017: fig. 49/h–n).

Genus *Allosminthus* WANG, 1985

Allosminthus cf. minutus (DAXNER-HÖCK, 2001)

(Fig. 10 B1–B2)

2001 *Heosminthus minutus* n. sp. – DAXNER-HÖCK: 363–365, pl. 2, figs 1–11, tabs 4–5.

2014 *Allosminthus minutus* (DAXNER-HÖCK, 2001) – DAXNER-HÖCK, BADAMGARAV & MARIDET: 140–142, fig. 5, tab. 3.

Material and measurements: 3 specimens; fragmentary left m1 (NHMW 2018/0034/0001), length 0.78 mm; left m2 (NHMW 2018/0034/0002), length 0.80 mm, width 0.66 mm; fragmentary right m2 (NHMW 2018/0034/0003), width 0.59 mm.

Main characteristics of the genus: The very small size of the teeth. The upper incisors have no longitudinal groove. The molar morphology resembles *Heosminthus*, except for some primitive characters of *Allosminthus*: *e. g.*, the crests and cusps are low and weak, the mesoloph(id) is frequently absent, and the anteroconid is weak or absent. *Allosminthus* is the smallest of all Dipodidae genera of the Oligocene of Asia.

Description: The teeth are smallest of all Dipodidae from the Shine Us assemblage. The m1 and m2 have two roots.

- ◀ Fig. 10. Dipodidae from the Shine Us locality (assemblage SHU-A/1), Khaliun Basin, south western Mongolia, Beger Fm., upper Oligocene. *Heosminthus chimidae*: **A1**: m1 left (NHMW 2018/0029/0058), **A2**: m2 left (NHMW 2018/0029/0088), **A3**: m3 left (NHMW 2018/0029/0108), **A4**: P4 (NHMW 2018/0029/0122), **A5**: M1 right (NHMW 2018/0029/0021), **A6**: M2 right (NHMW 2018/0029/0040), **A7**: M3 left (NHMW 2018/0029/0043), **A8**: M1 right, lingual (NHMW 2018/0029/0019). *Allosminthus cf. minutus*: **B1**: m1 left (NHMW 2018/0034/0001), **B2**: m2 left (NHMW 2018/0034/0002). *Bohlinosminthus parvulus*: **C1**: m1 left (NHMW 2018/0033/0025), **C2**: m2 left (NHMW 2018/0033/0049), **C3**: m3 right (NHMW 2018/0033/0041), **C4**: M1 left, lingual (NHMW 2018/0033/0004), **C5**: P4 (NHMW 2018/0033/0046), **C6**: M1 left (NHMW 2018/0033/0001), **C7**: M2 left (NHMW 2018/0033/0011), **C8**: M3 left (NHMW 2018/0033/0019). *Litodonomys* sp.: **D1**: M2 left frag. (NHMW 2018/0030/0001), **D2**: M3 right (NHMW 2018/0030/0002). *Parasminthus tangingoli*: **E1**: m1 right (NHMW 2018/0031/0029), **E2**: m2 right (NHMW 2018/0031/0036), **E3**: m3 left (NHMW 2018/0031/0043), **E4**: M1 right, lingual (NHMW 2018/0031/0005), **E5**: P4 right (NHMW 2018/0031/0048), **E6**: M1 left (NHMW 2018/0031/0002), **E7**: M2 right (NHMW 2018/0031/0016), **E8**: M3 right (NHMW 2018/0031/0022). *Parasminthus cf. asiaecentralis*: **F1**: P4 (NHMW 2018/0032/0016), **F2**: M1 left (NHMW 2018/0032/0002), **F3**: m2 left (NHMW 2018/0032/0007). All right side specimens are inverted and the numbers underlined.

m1: It has a weak anteroconid. The protoconid and metaconid are in opposite position and are connected by a short metalophid. The hypolophid is transverse and extends to the anterior arm of the hypoconid. There is no mesolophid, but a weak mesoconid is present at the short ectolophid.

m2: It is rectangular in occlusal outline. Anterior and posterior conids are in alternating position. The short metalophid and hypolophid connect with the anterior arms of the protoconid and hypoconid, respectively. There is no mesolophid. The posterolophid is the most prominent lophid. The posterior sinusid is located between the hypoconid and the hypoconulid at the posterior wall of m2.

Remarks: The very small size and the molar pattern agrees with the genus *Allosminthus* from Shine Us. The scarce material does not allow sure species identification, however, the three available lower teeth correspond with *A. minutus* from the lower Oligocene of the type locality Hsanda Gol (level: SHG-A/20) (DAXNER-HÖCK 2001) and neighbouring regions of the Valley of Lakes. The stratigraphic range is letter zone B to C in Mongolia.

Genus *Bohlinosminthus* LOPATIN, 1999

***Bohlinosminthus parvulus* (BOHLIN, 1946)**

(Fig. 10 C1–C8, Tab. 8)

1946 *Parasminthus parvulus* n. sp. – BOHLIN: 30–41, figs 2/11–23, 30, 33, 36; 3/7–28; 4/1–4; 5C, 6C; pl. I, figs 4, 5, 10, 12, 15, 16, 20, 21.

2014 *Bohlinosminthus parvulus* (BOHLIN, 1946) – DAXNER-HÖCK, BADAMGARAV & MARIDET: 178–181, figs 18/1–23, tab. 14.

Material: 49 isolated teeth; 4 P4 (NHMW 2018/0033/0044–0047), 5 M1 left (NHMW 2018/0033/0001–0005), 5 M1 right (NHMW 2018/0033/0006–0010), 4 M2 left (NHMW 2018/0033/0011–0014), 4 M2r right (NHMW 2018/0033/0015–0018), 4 M3 left (NHMW 2018/0033/0019–0022), 1 M3 right (NHMW 2018/0033/0023),

Table 8. Descriptive statistics of tooth measurements of *Bohlinosminthus parvulus* from assemblage SHU-A/1, locality Shine Us, Khaliun Basin, south western Mongolia.

	length (mm)			width (mm)	
	range	mean	n	range	mean
P4	0.47–0.54	0.50	4	0.47–0.54	0.50
M1	0.87–0.94	0.90	9	0.71–0.82	0.79
M2	0.75–0.92	0.84	8/7	0.71–0.85	0.80
M3	0.60–0.68	0.64	4	0.59–0.75	0.70
m1	0.87–0.96	0.92	9	0.64–0.71	0.68
m2	0.85–0.96	0.91	5	0.68–0.78	0.73
m3	0.73–0.82	0.76	7	0.56–0.66	0.62

4 m1 left (NHMW 2018/0033/0024–0027), 5 m1 right (NHMW 2018/0033/0028–0032), 4 m2 left (NHMW 2018/0033/0033–0034, 2018/0033/0048–0049), 1 m2 right (NHMW 2018/0033/0035), 3 m3 left (NHMW 2018/0033/0036–0038), 5 m3 right (NHMW 2018/0033/0039–0043).

Measurements: see Tab. 8.

Main characteristics of the genus: The size of the molars is small. The upper incisors have no longitudinal groove. The upper M1–2 have square, the lower m1–2 rectangular occlusal outline (similar with *Heosminthus*). The bunodont molars have pronounced crests and cusps. The main differences from *Heosminthus* are: the small size, the reduction of protoloph II of M2, and the posterior arm of the protoconid of m2 dominates over the mesolophid. M1 and M2 have predominantly four rounded roots, whereas M1 and M2 of *Heosminthus* have three roots (one wide lingual and two rounded labial roots).

Description: P4: one cusp is surrounded by a posterior cingulum.

M1–2: They are trapezoidal to almost square in occlusal outline. Labially the teeth are wider than lingually. They have four main cusps in opposite position. Mesoloph is long, protoloph and metaloph are single. Only one M2 has a short mesoloph and a double protoloph. There is no posterior sulcus of M1. Metaloph of M1 joins hypocone. Metaloph of M2 joins entoloph anterior to hypocone. M1–2 have four or three roots. In the case of three roots the lingual root is flat, antero-posteriorly enlarged and its tips are split.

M3: It is the smallest upper molar. Sinus is closed, lophes are of varying length and number. M3 has three roots.

m1–2: They are rectangular in outline and have two roots. Anteroconid of m1 is weak, mesolophid long, ectolophid slightly oblique. Most m2 have a long posterior arm of protoconid, one a long mesolophid, and only one m2 shows both mesolophid and posterior arm of protoconid.

Remarks: The dental morphology and size of *B. parvulus* from Shine Us widely agrees with the type specimens from Tabenbuluk in China (BOHLIN 1946), and also with the rich material from the Taatsiin Gol and Taatsiin Tsagaan Nuur region in Mongolia (DAXNER-HÖCK *et al.* 2014: pp. 178–181, fig. 18, tab. 14), where the species is most abundant in the upper Oligocene (letter zones C and C1).

Genus *Litodonomys* WANG & QIU, 2000

***Litodonomys* sp.** (Fig. 10 D1–D2)

2000 *Litodonomys* gen. nov. – WANG & QIU: 1, 25.

2014 *Litodonomys* WANG & QIU, 2000. – DAXNER-HÖCK *et al.*: 181–190, figs 19–21, tabs 15–16.

Material and measurements: 2 specimens; fragmentary left M2 (NHMW 2018/0030/0001), length 1.08 mm, width 1.13 mm; right M3 (NHMW 2018/0030/0002), length 0.56 mm, width 0.71 mm.

Main characteristics of the genus: The molars have medium size, a plane occlusal surface, a very low crown, bulbous main loph(ids) and cones(ids), and a very thick enamel. The M1–2's are almost square in occlusal outline and have four roots. The M3 is very short, but wide. The upper incisors have no longitudinal groove.

Description: M2: The occlusal outline is anteriorly wider than posteriorly. The labial cusps are transversely elongate, the protocone is postero-lingually elongate, and the hypocone is in postero-lingual position. The lingual anteroloph is absent, the labial one long and extends to the labial margin. The protoloph and the metaloph are transverse, the entoloph is short, no mesoloph is present. The tooth is fragmentary in its postero-labial part. The sinus is narrow and oblique. No roots are preserved.

M3: It is very short, almost triangular in outline and with rounded corners. The protoloph and the metaloph enclose the fossette II+III. The entoloph, the mesoloph, the posteroloph and the lingual anteroloph are absent. The labial anteroloph is narrow and transversally aligned.

Remarks: The molar morphology of the material from Shine Us is in agreement with the genus *Litodonomys* from several Valley of Lakes localities (DAXNER-HÖCK *et al.* 2014: pp.181–182, figs 19–21, tabs 15–16), but it is too poor for species identification. The type material described by WANG & QIU (2000) from GL 9601B (Gansu, China) provides upper molars only. However, the rich material from the Valley of Lakes in Mongolia includes skulls, the upper and lower dentition, and therefore an emended diagnosis was possible (DAXNER-HÖCK *et al.* 2014: p.181). In Mongolia the stratigraphic range of *Litodonomys* is upper Oligocene to lowermost Miocene (letter zones C to D).

Genus *Parasminthus* BOHLIN, 1946

***Parasminthus tangingoli* BOHLIN, 1946**

(Fig. 10 E1–E8, Tab. 9)

1946 *Parasminthus tangingoli* n. sp. – BOHLIN: 23–30, figs 2/7–10, 3/1–6, 28, 31–45, 5B, 6B; pl. I, figs 3, 7–9, 11.

2000 *Parasminthus tangingoli* BOHLIN, 1946 – WANG & QIU: 15–17, fig. 1, tab. 1.

Material: 52 isolated teeth/partly fragmentary; 5 P4 (NHMW 2018/0031/0048–0052), 4 M1 left (NHMW 2018/0031/0001–0004), 4 M1 right (NHMW 2018/0031/0005–0008), 7 M2 left (NHMW 2018/0031/0009–0015), 5 M2 right (NHMW 2018/0031/0016–0020), 1 M3 left (NHMW 2018/0031/0021), 5 M3 right (NHMW 2018/0031/0021–0025), 3 m1 left (NHMW 2018/0031/0026–0028), 4 m1 right (NHMW 2018/0031/0029–0032), 2 m2 left (NHMW 2018/0031/0033–0034), 6 m2 right (NHMW 2018/0031/0035–0040), 6 m3 left (NHMW 2018/0031/0041–0046), 1 m3 right (NHMW 2018/0031/0047).

Measurements: see Tab. 9.

The main characteristics of the genus: The upper incisors have no longitudinal groove. The size of the molars is medium to large. Upper M1–2 and lower m1–2

are rectangular in occlusal outline. M1–2 have four, M3 three, and m1–3 two roots. The M1 has a protoloph II and a metaloph II, the M2 have double protolophs. The metaloph II is directed backwards and joins the hypocone or its posterior arm. The posterior sulcus between the hypocone and the posteroloph of M1 is a main characteristic of the genus.

Description: P4: It consists of an anterior cone and a posterior cingulum partly surrounding the cone.

M1–2: They are rectangular in occlusal outline. They have a long mesoloph, a shallow forward-directed sinus and four roots.

M1: In most cases M1 has a long anterior arm of the protocone. It has a single protoloph, and the metaloph joins the hypocone or its posterior arm. The posterior sulcus between the hypocone and the posteroloph is pronounced or weak.

M2: It has a strong labial and a weak lingual anteroloph. The protoloph is double (five specimens), in all other specimens the posterior protoloph is weak, constricted or absent. The metaloph joins the hypocone or its anterior arm. A posterior sulcus is absent or weak.

M3: It is the smallest upper molar, with rounded outline, a closed sinus and three roots.

The lower molars are rectangular in outline and have two roots.

m1: The anteroconid of m1 is weak. The mesolophid is long, sometimes of medium length, or absent. The ectolophid is oblique. Some specimens display a small hypoconulid and a weak posterior sinusid.

m2: The metalophid and the hypolophid of m2 are directed forward. The posterior arm of the protoconid is frequently present, the mesolophid is weak or absent.

m3: It resembles m2, but is posteriorly narrowed.

Remarks: Apart from minor morphological variations, the molar pattern and size of the Shine Us specimens are in agreement with the type material from the upper

Table 9. Descriptive statistics of tooth measurements of *Parasminthus tangingoli* from assemblage SHU-A/1, locality Shine Us, Khaliun Basin, south western Mongolia.

	length (mm)			width (mm)	
	range	mean	n	range	mean
P4	0.71–0.80	0.76	5	0.71–0.80	0.76
M1	1.29–1.44	1.35	6/8	0.99–1.18	1.10
M2	1.20–1.34	1.28	9/10	1.01–1.15	1.09
M3	0.92–1.01	0.96	5	0.96–1.04	1.01
m1	1.22–1.39	1.32	3/6	0.94–1.15	1.00
m2	1.18–1.34	1.26	8	0.94–1.06	0.98
m3	1.06–1.27	1.17	5	0.89–1.04	0.97

Oligocene of Tabenbuluk in China (BOHLIN 1946). They also resemble the specimens from the upper Oligocene of Yindirte (WANG 2003), from GL 9601B Shangxigou in Gansu (China) (WANG & QIU 2000: tab. 1, fig. 1A+B), and a part of *P. tangingoli* from Ulantatal (China) (HUANG 1992: 277–279, pl. 3; revision by WANG & QIU 2000: 15–19). Moreover, they are quite similar to specimens described as *P. cf. tangingoli* from five upper Oligocene deposits (letter zones C and C1) of the Taatsiin Gol and Tatal Gol regions in Mongolia (DAXNER-HÖCK *et al.* 2014: tab. 12, fig. 16). All Cenozoic Mongolian assemblages provide associations of *P. tangingoli* / *P. cf. tangingoli*, *P. cf. asiaecentralis* and *B. parvulus*.

***Parasminthus cf. asiaecentralis* BOHLIN, 1946**

(Fig. 10 F1–F3, Tab. 10)

1946 *Parasminthus asiae-centralis* n. sp. – BOHLIN: 18–22, figs 2/1–6, 3/28–30, 5A, 6A; pl. I, figs 2, 6, 13, 14.

2000 *Parasminthus asiae-centralis* BOHLIN, 1946 – WANG & QIU: 14–15, fig. 1.

Material: 19 isolated teeth / partly fragmentary; 6 P4 (NHMW 2018/0032/0014–0019), 3 M1 left (NHMW 2018/0032/0001–0003), 1 M2 left (NHMW 2018/0032/0004), 2 M3 left (NHMW 2018/0032/0005–0006), 5 m2 left (NHMW 2018/0032/0007–0011), 1 m2 right (NHMW 2018/0032/0012), 1 m3 left (NHMW 2018/0032/0013).

Measurements: see Tab. 10.

Remarks: Most teeth are strongly damaged and do not allow reliable description of dental characters. However, tooth size and the overall dental morphology are in agreement with the type material of *P. asiaecentralis* from Tabenbuluk (BOHLIN 1946), known to be the largest *Parasminthus* species. As shown above, co-occurrences of the smaller species *P. tanginogli* and the larger *P. asiaecentralis* are known from upper Oligocene assemblages of Mongolia and China. *P. tangingoli* and *P. cf. asiaecentralis* differ from other Dipodidae from Shine Us by larger size and the rectangular shape of upper and lower molars.

Table 10. Descriptive statistics of tooth measurements of *Parasminthus cf. asiaecentralis* from assemblage SHU-A/1, locality Shine Us, Khaliun Basin, south western Mongolia.

	length (mm)		n=14 n	width (mm)	
	range	mean		range	mean
P4	0.89–1.04	0.97	6	0.89–1.04	0.94
M1	1.53–1.93	1.67	3	1.36–1.58	1.44
M3	1.29–1.36		2		1.18
m2	1.69–1.81		3	1.27–1.46	1.44

Ruminantia (B. MENNECART)

Nomenclature, measurements and dental terminology of Ruminantia: Postcranial bones after BARONE (1999), metapodials and phalanges after KÖHLER (1993), astragalus after MARTINEZ & SUDRE (1995) and dental terminology after BÄRMANN & RÖSSNER (2011). The bodymass estimation is based on the astragalus after MARTINEZ & SUDRE (1995), on the radius after SCOTT (1990) and on the upper molars after JANIS (1990). Environmental characters of the postcranial bones are based on KÖHLER (1993). Tragulina is here considered to be a “non-pecoran ruminant.”

Cetartiodactyla MONTGELARD, CATZEFLIS & DOUZERY, 1997

Ruminantia SCOPOLI, 1777

Tragulina FLOWER, 1883

Tragulina indet.

(Fig. 11 A–M, Tab. 11)

Material: Astragalus right (NHMW 2018/0028/0001–0005), astragalus left (NHMW 2018/0028/0006), fibula left (NHMW 2018/0028/0007), cubonavicular right (NHMW 2018/0028/0008), metapod distal part, fragments (NHMW 2018/0028/0009–0010), proximal phalanx (NHMW 2018/0028/0011–0012), middle phalanx (NHMW 2018/0028/0013), distal phalanx (NHMW 2018/0028/0014–0016), central phalanx (NHMW 2018/0028/0017), lateral phalanx (NHMW 2018/0028/0018), radius proximal part right (NHMW 2018/0028/0019), upper fourth premolar right (NHMW 2018/0028/0020), fragmented upper molar right (NHMW 2018/0028/0021).

Measurements: see Tab. 11.

Equation bodymass based on the astragalus (MARTINEZ & SUDRE 1995: L length and W width of the astragalus; size in mm and result in gram):

$$\text{Bodymass} = 3.16 \times (L \times W)^{1.482}; (R^2 = 0.95)$$

Table 11. Astragalus measurements of *Tragulina indet.* from Shine Us (assemblage SHU-A/1) and bodymass estimation based on astragalus.

Inv. No.	L	W	Body mass (kg)
NHMW 2018/0028/0003	18.00	10.60	7.60
NHMW 2018/0028/0004	17.30	9.70	6.30
NHMW 2018/0028/0002	19.30	10.70	8.50
NHMW 2018/0028/0005	17.50	10.00	6.70
NHMW 2018/0028/0001	18.60	10.60	7.90

Equation bodymass based on the radius (SCOTT 1990: R2, distal radius length; R3, distal radius width; size in cm and result in kg): see Tab. 12.

Ungulates

$$\text{Log Body} = \text{Log (R2)} \times 2.4304 + 0.4856; (R^2=0.9494)$$

$$\text{Log Body} = \text{Log (R3)} \times 2.5360 + 1.0605; (R^2=0.9381)$$

Artiodactyls

$$\text{Log Body} = \text{Log (R2)} \times 2.4768 + 0.9478; (R^2=0.9478); \text{Log Body} = \text{Log (R3)} \times 2.5374 + 1.0603; (R^2=0.9321)$$

Ruminants

$$\text{Log Body} = \text{Log (R2)} \times 2.5149 + 0.4297; (R^2=0.9638); \text{Log Body} = \text{Log (R3)} \times 2.5443 + 1.0519; (R^2=0.9339)$$

Equation bodymass based on the upper molar length (JANIS 1990: size in cm and result in kg):

$$\text{Ungulates: Log Body} = \text{Log (SUML)} \times 3.184 + 1.091; (R^2=0.932)$$

$$\text{Ruminants: Log Body} = \text{Log (SUML)} \times 3.337 + 1.118; (R^2=0.939)$$

Description: Astragalus: The astragalus is relatively slender. The trochleas are unaligned. Moreover, the lateral condyles of the trochleas are more developed (larger and higher) than the medial ones. The surface of the proximal trochlea is more concave than the distal one. The bone shows a general asymmetry. The astragalo-calcaneal contact is widely laterally projected. The posterior calcaneal lateral facet, laterally projected, stops almost at the mid-height of the bone. No crest separates the articular surface of the cuboid and the navicular surface on the distal trochlea and in the medial ridge of the sustentacular facet because these two bones are fused. The contact with the cubonavicular also stops at mid-height of the sustentacular facet and forms an incipient crest on the medial view. The sustentacular facet is not centered with the astragalus. The contact with the internal malleolus is shallow, rounded, and open on its plantar section. The medial part of the proximal trochlea bears a crest, which is absent on the lateral one.

Fibula: The fibula is reduced to its distal extremity only. This bone is quadrangular in shape (length: 8.5mm, height: 6.3mm) and very-flattened (width: from 2.4 to 4.2 mm). The proximal part that articulates with the tibia bears a developed bony-spine. The distal surface, articulating with the calcaneum, is slightly concave. The internal surface shows

Table 12. *Tragulina* indet. from Shine Us (assemblage SHU-A/1); bodymass estimates based on the radius (SCOTT 1990).

Bodymass (kg)	Ungulates	Artiodactyls	Ruminants
R2	7.17	7.00	7.51
R3	6.32	6.32	6.19

a shallow curved surface of contact with the astragalus, whereas the outer surface is relatively flattened.

Cubonavicular: The cubonavicular is massive (height: 12.6, length: 12.7, width: 12.7 mm). The cuneiform surface contact shows that this bone was relatively high. The articular surface with the astragalus is high, and asymmetrical due to the shape of the astragalus. The articular surface with the calcaneum is oblique, elongated and deeply marked. The plantar surface is not flattened.

Metapodial bones: The distal part of the metapods, somewhat enlarged compared with the diaphysis, is not fully fused, thus forming an open gully on its distal part. The specimens lack crests on both side of the sulcus. The distal part of the articular surface is flattened and the keel does not reach the dorsal part of the metapod. In lateral view, the dorsal part is slightly convex.

Proximal phalanx: The proximal phalanx is relatively robust. No central sulcus is visible on the broad proximal articular surface. This facet is very rounded. The dorsal surface outline is slightly convex. The area for the insertion of the interdigital ligament is broad (half of total phalanx length). The plantar side shows a double concave volar curvature. The central ligament insertion area is well marked, forming the second curvature. The distal articular facet is visible from dorsal view and is rounded from the side view.

Middle phalanx: The middle phalanx is strong. The proximal and distal articular surfaces are of similar size. In lateral view, the proximal facet is very flattened. The postarticular plateau is proximally elongated with a strongly marked origin of the interdigital ligaments on the proximal volar end. In plantar view, two crests are visible on the proximal part due to the insertion of the collateral ligaments. The dorsal extensor process is very reduced. The distal articular surface extends somewhat dorsally. In lateral view, the distal end of the phalanx is ovoid.

Distal phalanx: The distal phalanx exhibits two different sizes. We attribute the smallest one to a lateral digit, while the largest ones are central digits. They are triangular. The central ones are massive, whereas the lateral ones are more acute angled. The dorsal ridge is straight, elongated, oriented toward the interdigital side, without any special process for the insertion of the extensor on its dorso-proximal part. The surface of the proximal articular is slightly concave. The wedge with a plantar process for the insertion of the deep flexor tendon is well developed on the central phalanges. The interdigital surface is flattened.

Radius: The narrow radius (R2: 1.42, R3: 0.79 cm) shows its proximal suture with the ulna. The tuberosity of the extensor muscle of the lateral digit is very well developed. The proximal area may be rectangular. The coronoid process is weakly developed, *e. g.*, the synovial depression of the radius, which only forms a fissure on the plantar side.

Upper fourth premolar: The very simplified upper fourth premolar is weakly asymmetrical. The tooth is as long as large (6.0 × 6.2 mm). The posterolingual and anterolingual cristae are straight and short. The labial cone and the lingual cone are positioned

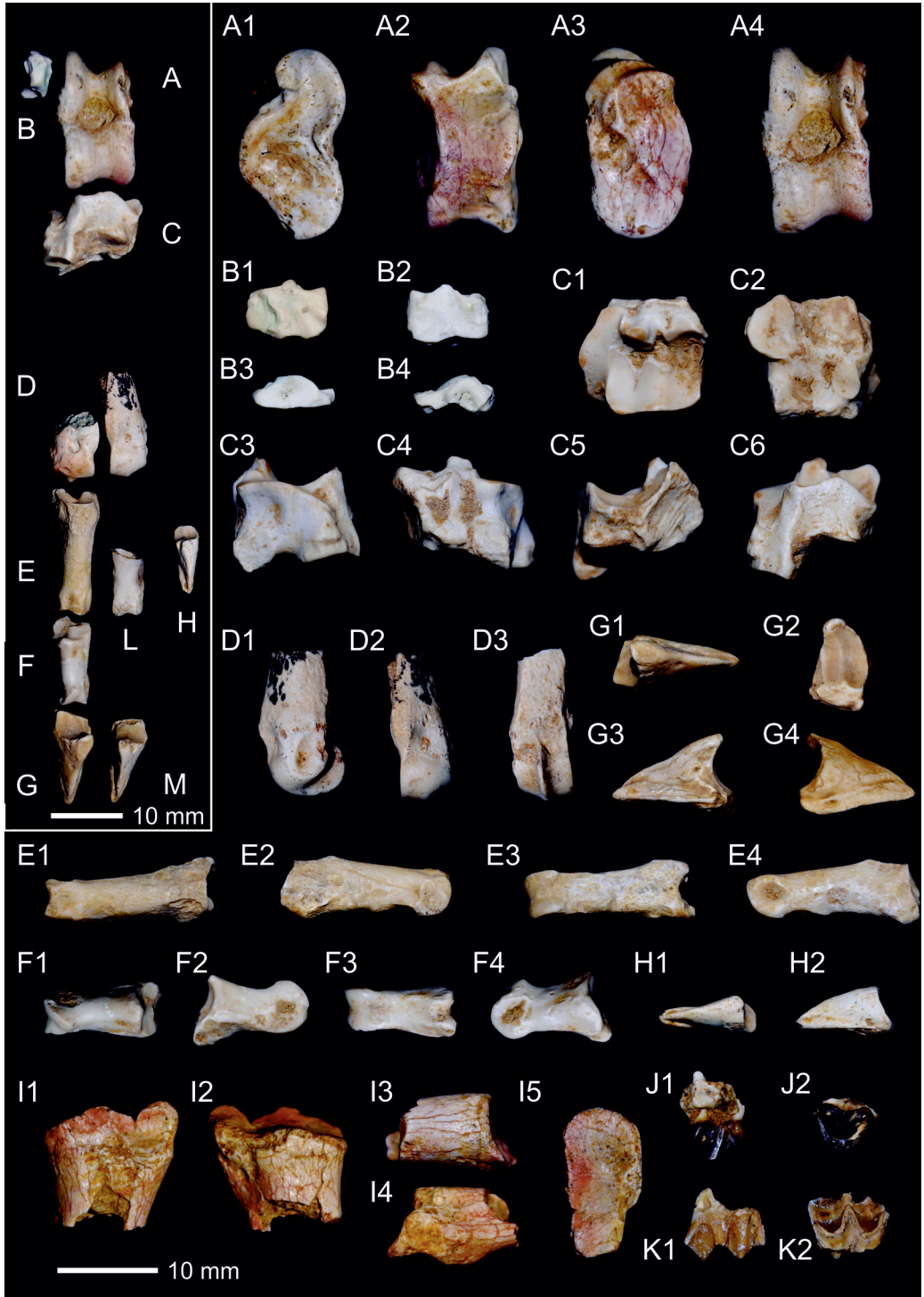
medially. The fossa lacks an additional fold. The labial cone rib is weak, whereas the anterior style and the posterior style are well developed (the anterior style being bigger). The labial cristae are slightly curved, giving a slightly concave aspect to the labial wall of the tooth.

Upper molar: The fragmented molar is very small (length 8.4 mm). The lingual and anterior parts of the solitary molar are broken. The premetaconulecrista is elongated and ends almost at the level of the mesostyle, between the paracone and metacone. The postproto-crista is short, stopping along the premetaconulecrista at its mid-length. The anterior and posterior fossae are small. The paracone and metacone are aligned. The paracone rib is very big, whereas the labial part of the metacone is flat. The labial cristae are short and straight. The metastyle is well developed, forming a labial crest. The mesostyle, even broken, is very big.

Taxonomic attribution: All studied specimens have a similar preservation status, size and morphological characteristics. We strongly suggest that these remains belong to only one ruminant species. Ruminants are already documented from the Shine Us locality (VISLOBOKOVA 1997: fig. 4), *i. e.*, *Palaeohypsodontus asiaticus* has been listed from fossil point Shine-Us 1, *Amphitragulus cf. gracilis* from Shine-Us 2. Nonetheless, the general morphology of the presently studied bones and teeth from sample SHU-A/1 recall the morphological characteristics of Tragulina. Contrarily to Pecora, the trochleas of the astragalus are unaligned and slender (MARTINEZ & SUDRE 1995; MENNECART *et al.* 2011).

Only few Oligocene ruminant astragali are currently described (MARTINEZ & SUDRE 1995; MÉTAIS *et al.* 2009, 2017; MENNECART 2015). The Shine Us (SHU-A/1) ruminant astragalus is very similar to those of the traguline *Bachitherium* in being slender, with unaligned trochleas and strong asymmetry between the trochleas (MARTINEZ & SUDRE 1995;

Fig. 11. Ruminant postcranial and dental remains from the Shine Us locality (assemblage SHU-A/1), Khaliun Basin, south western Mongolia, Beger Fm., upper Oligocene. **A:** astragalus (NHMW 2018/0028/0001), lateral (A1), plantar (A2), medial (A3), and dorsal (A4) views; **B:** cubonavicular (NHMW 2018/0028/0008) in proximal (B1), distal (B2), lateral (B3), plantar (B4), medial (B5), and dorsal (B6) views; **C:** fibula (NHMW 2018/0028/0007) in lateral (C1), medial (C2), proximal (C3), and distal (C4) views; **D:** metapodial (NHMW 2018/0028/0009) in lateral (D1), dorsal (D2), and plantar (D3) views; **E:** proximal phalanx (NHMW 2018/0028/0011) in dorsal (E1), lateral (E2), plantar (E3), and medial (E4) views; **F:** middle phalanx (NHMW 2018/0028/0013) in dorsal (F1), lateral (F2), plantar (F3), and medial (F4) views; **G:** distal central phalanx (NHMW 2018/0028/0014) in dorsal (G1), proximal (G2), lateral (G3), and medial (G4) views; **H:** distal lateral phalanx (NHMW 2018/0028/0018) in dorsal (H1) and lateral (H2) views; **I:** radius (NHMW 2018/0028/0019) in dorsal (I1), plantar (I2), lateral (I3), medial (I4), and proximal (I5) views; **J:** upper fourth premolar (NHMW 2018/0028/0020) in labial (J1) and occlusal (J2) views; **K:** upper molar (NHMW 2018/0028/0021) in labial (K1) and occlusal (K2) views; **L:** proximal phalanx (NHMW 2018/0028/0012) in dorsal view; **M:** distal central phalanx (NHMW 2018/0028/0015) in dorsal view. Scale bar: 1 cm. ►



MENNECART 2015). The contact with the cubonavicular also stops at mid-height of the sustentacular facet and forms an incipient crest in medial view, and the sustentacular facet is not centered with the astragalus (MARTINEZ & SUDRE 1995; MENNECART 2015). The metapodial bones and phalanges also recall the condition observed in the traguline *Bachitherium* and *Dorcatherium*, the articular surfaces being smooth without acute keels or convex surfaces (BLONDEL 1997; MENNECART *et al.* 2018b). They could, however, also be ecomorphologic characteristics (KÖHLER 1993). The symmetry of the upper fourth premolar, the shortened cristae and the aligned labial cusps are also known in Tragulina. Based on these characters, we the ruminant from the Shine Us (SHU-A/1) to the Tragulina. Further determination is currently impossible because of the scarcity of the material.

The early diversification of ruminants (Tragulina only) occurred during the middle and upper Eocene in Asia, northern America, and eastern Europe (MÉTAIS & VISLOBOKOVA 2007; MENNECART *et al.* 2018a). The Tragulina dominated the ruminant fauna in Asia and Europe during the lower Oligocene, and persisted to the uppermost Oligocene south of the Himalaya and in Europe (VISLOBOKOVA 1997; VISLOBOKOVA & DAXNER-HÖCK 2002; MENNECART 2012; SCHERLER *et al.* 2013; MENNECART 2015; MÉTAIS *et al.* 2017). So far only Pecora were known from the upper Oligocene and lower Miocene of the Valley of Lakes and the Khaliun Basin in Mongolia (VISLOBOKOVA 1997; VISLOBOKOVA & DAXNER-HÖCK 2002). Nonetheless, the new findings from Shine Us (sample SHU-A/1) demonstrate that the environmental conditions of the Khaliun Basin allowed Tragulina to survive from the lower Oligocene to the basal upper Oligocene.

Palaeoecological and palaeoenvironmental indications: Very little is known about the palaeoecology of Paleogene ruminants, specifically in Asia.

Bodymass: From living “ungulates”, strong correlations between body size and diet are known, *e. g.*, most of the living small ruminants (less than 20 kg) are selective browsers (DEMMENT & SOEST 1985; BODMER 1990; MENNECART *et al.* 2012a). Due to the short retention time of the food in the digestive system and a proportionally higher metabolic rate, small-size ruminants are mostly selective browsers feeding on “high-quality” energetic food such as fruits and living in closed environments such as forests (BODMER 1990). The estimated bodymass of Oligocene European ruminants is mostly less than 20 kg (MARTINEZ & SUDRE 1995; BLONDEL 1998), except for the slightly larger *Lophiomeryx* and *Prodremotherium* (respectively 29 kg and 21 kg). Based on mandibular morphology (MENNECART *et al.* 2011, 2012a, MENNECART 2012), microwear analyses (BLONDEL 1996, NOVELLO *et al.* 2010) and isotopic data (BLONDEL 1996; ZANAZZI & KOHN 2008), the diet of some species from the Oligocene of Europe and Eocene-Oligocene of northern America has been defined. Except for Pecora from the latest Oligocene of La Milloque (*ca.* 23.5 Ma, France), ruminants were not pure grazers or mixed-feeders during the Oligocene (NOVELLO *et al.* 2010).

The bodymass of the Shine Us (SHU-A/1) Tragulina, estimated from the astragali (6.3 kg to 8.5 kg, mean 7.4 kg), from the radius (6.2 kg to 7.5 kg, mean 6.8 kg) and from the

upper molar (7.1 kg to 7.3 kg, mean 7.2 kg), indicates a bodymass of about 7 kg. Accordingly, we consider it to have been mainly a selective browser, similarly to its European contemporaneous relatives and to living Tragulidae (SUDRE 1984; NOWAK 1999; MENNECART *et al.* 2011, 2012a). Its bodymass indicates a forested environment in Shine Us. Postcranial elements of Ruminantia provide valuable information about palaeoenvironmental conditions, such as: wooded and moderately humid; wooded and very humid to semi-aquatic; open, flat and dry; mountainous (KÖHLER 1993). Using these morphoecological characteristics, habitat preferences have been elaborated for European Oligo-Miocene ruminants (BLONDEL 1997; BECKER *et al.* 2010; MENNECART *et al.* 2012b).

Postcranials: Considering the postcranial elements of specimens from SHU-A/1, the tuberosity of the extensor muscle of the lateral digit is very well developed on the radius. The lateral distal phalanx size indicates that the lateral digit was well developed. It provides a high mobility of the lateral digits and a high lateral stability necessary on unstable soil (swamp). It is in agreement with the morphology of phalanges and metapodial bones, which are also typical for a wet and wooded environment. Indeed, the robustness of the phalanges along with concave outline, the absence of very marked keels or grooves on the articulation surfaces, and the presence of strong insertions for interdigital ligaments are typical for the animals living in wooded environments (KÖHLER 1993). The absence of crests on both sides of the sulcus of the metapods is known only in animals living in very humid environments (KÖHLER 1993). The postcranial elements of the ruminant from Shine Us (SHU-A/1) are typical for animals living in a very humid forest. These data confirm the palaeoenvironmental conditions deduced from the bodymass.

Discussion

Biostratigraphy

For a better understanding of the biostratigraphy of the Shine Us assemblage, we refer to previous investigations in the Taatsiin Gol and Taatsiin Tsagaan Nuur regions (Valley of Lakes). There, >70 palaeontological samples were collected from 30 sections and natural outcrops of Oligocene and Miocene deposits of the Hsanda Gol and Loh formations. The huge dataset of mammal fossils enabled establishing informal letter zones for the Oligocene and Miocene (letter zones A to E) (DAXNER-HÖCK *et al.* 1997; HÖCK *et al.* 1999). Later, the refined letter zones A, B, C, C1, C1–D of the Oligocene, and letter zone D of the lowermost Miocene (DAXNER-HÖCK *et al.* 2017) were defined as “**Taxon Range Zones**” and “**Abundance Zones**” (HARZHAUSER *et al.* 2017). “**Taxon Range Zones**” are based on the lowest and highest occurrences of taxa (= LO-HO) and “**Abundance Zones**” are based on the most abundant/frequent occurrences of taxa (= AO) according to the International Stratigraphic Guide (HARZHAUSER *et al.* 2017).

The fossil composition of the Shine Us sample SHU-A/1 from the Beger Fm. is broadly in agreement with the “***Ampechinus taatsiingolensis* Abundance Zone**” (= letter zone C)

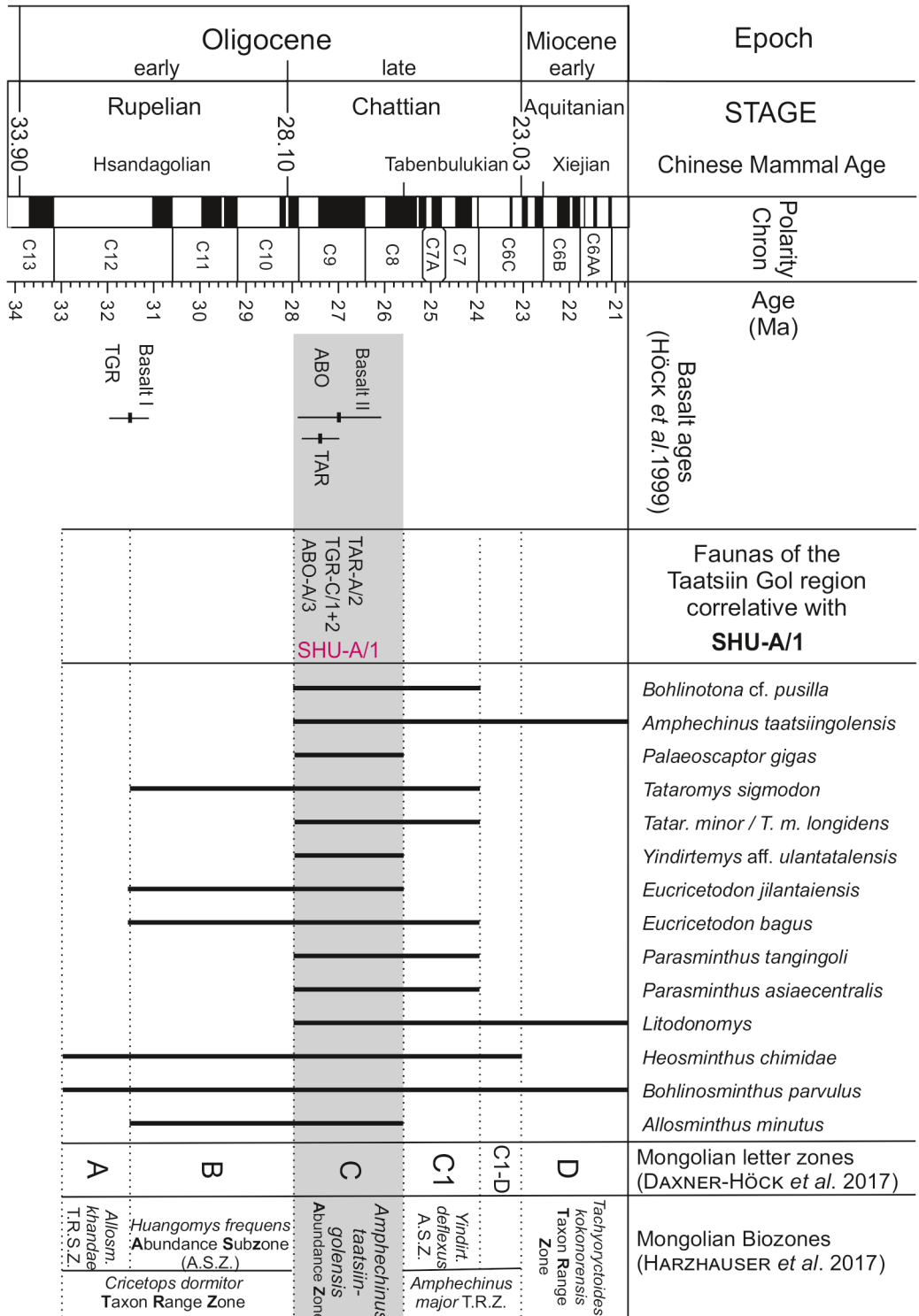
of the Valley of Lakes. This zone was defined by HARZHAUSER *et al.* (2017) by the “lowest occurrence” (LO) and the very frequent occurrence (AO) of *Amphechinus taatsiingolensis*. Other “lowest occurrences” from the Valley of Lakes localities are: *Bohlinotona cf. pusilla*, *Palaeoscaptor gigas*, *Tataromys minor*, *Parasminthus cf. tangingoli*, *Parasminthus cf. asiaecentralis*, *Yindirtemys aff. ulantatalensis* and the genus *Litodonomys*. In addition, *Eucricetodon bagus*, *Eucricetodon jilantaiensis*, *Tataromys sigmodon*, and *Tataromys minor* are very abundant, and *E. jilantaiensis*, *Palaeoscaptor gigas*, *Yindirtemys aff. ulantatalensis*, and *Allosminthus minutus* have “highest occurrences” (HO) in this Biozone (HARZHAUSER *et al.* 2017; LÓPEZ- GUERRERO *et al.* 2017a; OLIVER *et al.* 2017; DAXNER-HÖCK *et al.* 2014, 2017; ERBAJEVA & DAXNER-HÖCK 2014; ZIEGLER *et al.* 2007).

Correlation

The composite age chronology of the Valley of Lakes (DAXNER-HÖCK *et al.* 2017) is based on biostratigraphy (HARZHAUSER *et al.* 2017), $^{40}\text{Ar}/^{39}\text{Ar}$ ages of basalts (HÖCK *et al.* 1999), and on magnetostratigraphic record of the Taatsiin Gol sections TGR-A and TGR-C (SUN & WINDLEY 2015). All these data enabled correlation of sections and fossil horizons with the Geomagnetic Polarity Time Scale (GPTS) (GRADSTEIN *et al.* 2012), and suggest an early Chattian age (early late Oligocene; ~ 28.0–25.6 Ma) of the “*Amphechinus taatsiingolensis* Abundance Zone”.

The mammal composition, specifically the most frequent species of the Shine Us assemblage SHU-A/1 (Tab. 13) agree biostratigraphically with three Valley of Lakes assemblages of the “*Amphechinus taatsiingolensis* Abundance Zone”, *i. e.*, TAR-A/2 from the locality Unzing Churum, ABO-A/3 from Abzag Ovo, and TGR-C/1+2 from Taatsiin Gol. The radiometric and magnetostratigraphic data, respectively, date the assemblages at: TAR-A/2: $<27.4 \pm 0.4$ Ma; ABO-A/3: $>27.0 \pm 0.9$ Ma; TGR-C/1+2: Chron C9n = ~ 26.4 – 27.4 Ma (DAXNER-HÖCK *et al.* 2017: fig. 30). Consequently, correlation with these three well dated assemblages from the Taatsiin Gol region suggests an age between 26 and 28 million years of the Shine Us assemblage SHU-A/1. We exclude any considerably older or younger age because neither the index fossils of the older “*Huangomys frequens* Abundance Subzone” (> 28 Ma; early Oligocene), nor of the younger “*Yindirtemys deflexus* Abundance Subzone” (< 25.6 Ma, late late Oligocene) are documented from sample SHU-A/1 (Fig. 12).

Fig. 12. The correlation chart includes the Geologic Time Scale and the Geomagnetic Polarity Time Scale (GPTS) (GRADSTEIN *et al.* 2012; OGG *et al.* 2014); the Chinese Mammal Ages Hsandagolian, Tabenbulukian, and Xiejian; $^{40}\text{Ar}/^{39}\text{Ar}$ Basalt ages (HÖCK *et al.* 1999); well-dated assemblages TAR-A/2, ABO-A/3, and TGR-C/1+2 of the Valley of Lakes that are correlative with the assemblage SHU-A/1 of the Khaliu Basin; the Mongolian letter zones and Biozones (DAXNER-HÖCK *et al.* 2017; HARZHAUSER *et al.* 2017). The stratigraphic ranges of 14 mammal taxa of the assemblage SHU-A/1 indicate the *Amphechinus taatsiingolensis* Abundance Zone and an early late Oligocene age. ►



Palaeoenvironment

In reconstructing the palaeoenvironment, we focus on lithologies and sediment structures of the Shine Us section and on the composition of the SHU-A/1 assemblage as described above.

The SHU-A/1 assemblage stems from the lower part of the Beger Fm. (unit 17), where fossils were imbedded in light brown, locally laminated clayey silt. The concentrations of disarticulated, mostly fragmentary bones and teeth are interpreted to be accumulations of small floodplain channels from different nearby habitats. The environment was a floodplain, where small rivers may have drained into low areas creating temporary ponds and swamps. More distantly, we assume wooded meadows, forests and also open areas.

The recovered fossil assemblage turned out to be very diverse (Tab. 13), representing different habitats of the floodplain ecosystem. Thus, temporary rivulets and ponds were inhabited by ostracods and fishes. Adjacent wet forests provided a suitable habitat for carnivorous birds, bats, and for the small ruminants, the Tragulina. The latter provide morphoecological characteristics on upper molars and postcranials, indicating that the body size of Tragulina from Shine Us was small (~7kg). Like extant Tragulina they were mainly selective browsers, and the foot was adapted to swampy environments (MENECAART, this paper). The rodent groups Eomyidae, Sciuridae, and Aplodontidae may have lived in trees and bushes. More open and dry areas – where the sunlight reaches the ground – were inhabited by lizards, snakes, and snails. Also ground dwelling lagomorphs, insectivores, and rodent groups, such as Dipodidae and Cricetidae lived in more or less open habitats. According to microwear analyses on the cricetid *Eucricetodon* (from the locality Ulantatal in China) the diet of *E. bagus* consisted of herbaceous and shrub plants, that of *E. jilantaiensis* was more fibrous plants (GOMES RODRIGUES *et al.* 2012 b). However, Tachyoryctoididae and Tsaganomyidae, two prominent and locally dominating rodents of the Oligocene Valley of Lakes faunas, are practically absent from sample SHU-A/1. Their partial subterranean lifestyle would require more dry conditions and a lower groundwater table (WESSELS *et al.* 2014; DAXNER-HÖCK *et al.* 2015), than was evidenced by the fossil content of the sample (sediment unit 17; Beger Fm.) of the Shine Us locality.

Palaeoclimate

In the foregoing chapters we showed, that the mammal composition of the Shine Us assemblage (SHU-A/1) is in agreement with the *Amphechinus taatsiingolensis* Abundance Zone of the basal late Oligocene. During this time interval a diversity drop in mammal communities coincided with a major turnover, termed the “Mid Oligocene Reorganisation”, as evidenced on the basis of the excellent mammal record from the Valley of Lakes localities (HARZHAUSER *et al.* 2016: fig. 3). These extinctions affected mainly rodents, ruminants and carnivores of the early Oligocene. Simultaneously, new small mammal genera and species originated. This Mid-Oligocene Reorganisation event

Table 13. Fossils from assemblage SHU-A/1, locality Shine Us, Khaliun Basin in south western Mongolia collected 1997 and 2001.

Fossil taxa from assemblage SHU-A/1	specimens (n)	Inventory numbers (coll. NHMW)
Ostracoda		
Cypridae and Candonidae	> 100	NHMW 2018/0035/0000
Gastropoda		
Pupilloidea indet.	Internal casts, shells (<10)	NHMW 2018/0196/0000
Pisces		
Cyprinidae indet.	vertebrae, pharyngeal teeth (few)	NHMW 2018/0197/0000
Reptilia		
Lacertidae indet.	incomplete dentaries (3)	NHMW 2018/0040/0001–0003
Serpentes indet.	neural arch (1)	NHMW 2018/0041/0001
Aves		
Accipitridae indet.	claw (1)	NHMW 2018/0135/0001
Aves indet.	bones (5), egg shells (>50)	NHMW 2018/0135/0000
Mammalia		
Lagomorpha		
<i>Bohlinotona cf. pusilla</i>	premolars, molars and deciduous teeth (220); incisors, tooth fragments (pl.)	NHMW 2013/0113/0001–0220 NHMW 2013/0113/0000
<i>Desmatolagus sp.</i>	m1–2 (1)	NHMW 2013/0172/0001
<i>Sinolagomys sp.</i>	P3, Inc. sup. (2)	NHMW 2013/0382/0001–0002
<i>Archaeolagus sp.</i>	M1 (1)	NHMW 2013/0171/0001
Erinaceomorpha and Soricomorpha		
Brachyericinae indet.	dentary incomplete (1)	NHMW 2018/0021/0001
<i>Palaeoscaptor cf. rectus</i>	fragmentary teeth (3)	NHMW 2018/0022/0001–0003
<i>cf. Palaeoscaptor gigas</i>	teeth (3)	NHMW 2018/0023/0001–0003
<i>Amphechinus taatsiingolensis</i>	teeth (92)	NHMW 2018/0024/0001–0092
Crocidosoricinae gen. et sp. indet.	teeth (4)	NHMW 2018/0025/0001–0004
Talpidae gen. et sp. indet.	incomplete dentary, tooth (2)	NHMW 2018/0026/0001–0002
Chiroptera		
<i>cf. Myotis horaceki</i>	tooth (1)	NHMW 2018/0027/0001
Rodentia		
Aplodontidae indet.	teeth; strongly worn, fragments (3)	NHMW 2018/0198/0000
Sciuridae indet.	fragmentary teeth (2)	NHMW 2018/0199/0000
Eomyidae indet.	tooth; strongly worn (1)	NHMW 2018/0200/0000
Tsaganomyidae indet.	teeth (2)	NHMW 2018/0201/0000
Mammalia indet.	tooth fragments (5)	NHMW 2018/0202/0000
Ctenodactylidae		
<i>Tataromys sigmodon</i>	premolars and molars (133)	NHMW 2017/0018/0001–0133
<i>Tataromys minor</i>	premolars and molars (141)	NHMW 2017/0019/0001–0141
<i>Yintirtemys cf. ulantatalensis</i>	dentary fragments and molars (10)	NHMW 2017/0020/0001–0010
Cricetidae		
<i>Witenia sp.</i>	molar (1)	NHMW 2018/0136/0001
<i>Eucricetodon asiaticus</i>	molars (4)	NHMW 2018/0139/0001–0004
<i>Eucricetodon jilantaiensis</i>	molars (47)	NHMW 2018/0137/0001–0047
<i>Eucricetodon bagus</i>	molars (54)	NHMW 2018/0138/0001–0054
Dipodidae		
<i>Heosminthus chimidae</i>	dentary fragments, molars and premolars (127)	NHMW 2018/0029/0001–0117 NHMW 2018/0029/0121–0127
<i>Allosminthus cf. minutus</i>	molars (3)	NHMW 2018/0034/0001–0003
<i>Bohlinosminthus parvulus</i>	premolars and molars (49)	NHMW 2018/0033/0001–0049
<i>Litodonomys sp.</i>	molars (2)	NHMW 2018/0030/0001–0002
<i>Parasminthus tangingoli</i>	premolars and molars (52)	NHMW 2018/0031/0001–0052
<i>Parasminthus cf. asiaecentralis</i>	premolars and molars (19)	NHMW 2018/0032/0001–0019
Ruminantia		
Tragulina indet.	postcranial bones, and teeth (21)	NHMW 2018/0028/0001–0021

coincides with the Oligocene Glacial Maximum of the global climate (HARZHAUSER *et al.* 2016: fig. 3). Although it is not reflected by the available geochemical and geophysical record from the Valley of Lakes, a change in climate may have caused the mammal turnover during the early late Oligocene, rather than tectonic processes, such as the uplift of the Tibetan Plateau (HARZHAUSER *et al.* 2016). The similar mammal community of assemblage SHU-A/1 suggests comparable climate conditions of the Khaliun Basin and the Valley of Lakes during the Mid Oligocene cooling periode.

Conclusions

Sporadic fossil finds from the Beger and Uush formations in the Khaliun Basin are already known from earlier geologic and stratigraphic investigations (for details see: LISKUN & BADAMGARAV 1977; DEVYATKIN 1981; VISLOBOKOVA 1997). Nonetheless, detailed investigations of specific fossil layers and faunal sequences are still lacking.

Here we provide information about a test sample from the Shine Us locality. The screen-washed sample of the Beger Fm. gives a good impression of the faunal composition, of the palaeoenvironment, and enables age estimation based on biostratigraphic correlation of the SHU-A/1 assemblage with well-dated mammal assemblages of the Valley of Lakes (DAXNER-HÖCK *et al.* 2017).

The assemblage includes ~ 40 vertebrate and several invertebrate taxa (Tab. 13) which inhabited different parts of a floodplain environment: Ostracods and fishes lived in rivulets and temporary ponds. Tragulina lived in floodplain meadows and swampy forests, and drier sunny areas were inhabited by most lagomorphs, ground-dwelling rodents, and insectivores, by snakes, lizards, birds and snails.

The assemblage is here correlated with the “*Amphechinus taatsiingolensis* Abundance Zone” (early late Oligocene, early Chattian). The estimated age is between 26 and 28 million years.

During this time interval a major faunal turnover took place in the Valley of Lakes. It was caused by a major extinction event of rodents, ruminants and carnivores towards the end of the early Oligocene (*Huangomys frequens* Abundance Subzone), followed by a recovery of new small mammal taxa at the beginning of the late Oligocene (*Amphechinus taatsiingolensis* Abundance Zone). This turnover is termed the “Mid-Oligocene Reorganisation” and coincides with the “Oligocene Glacial Maximum” of the global climate (HARZHAUSER *et al.* 2016).

The main faunistic difference between the SHU-A/1 fauna and time equivalent faunas of the Valley of Lakes (~ 500 km towards east) is the presence of freshwater Ostracoda, Pisces, and Tragulina, and the absence of Tsaganomyidae and Tachyoryctoidae. This suggests locally wetter environmental conditions in the Khaliun Basin than observed in time-equivalent locations of the Taatsiin Gol and Taatsiin Tsagaan Nuur region (Valley of Lakes).

Acknowledgements

This research was supported by projects of the Austrian Science Fund (FWF): P-10505-GEO and P-23061-N19 to G.D.-H., and by the Swiss National Science Foundation projects P300P2_161065 & P3P3P2_161066 to S.M.

We thank our Mongolian and European partners for manifold support, specifically D. BADAMGARAV† who guided the excursions 1997 and 2001 to the Beger and Khaliun Basins, and N. ICHINOROV and B. BAYARMAA who organized and accompanied the excursion 2015. P. SZIEMER helped sorting the wet screened residuals. D. DANIELOPOL provided information about Ostracoda, O. SCHULTZ identified the fish fossils as vertebrae and pharyngeal teeth of Cyprinidae, and T. NEUBAUER attributed the badly preserved Gastropoda remains to Pupilloidea. SEM images were taken by D. GRUBER (Biocenter, University of Vienna), P. VALVERDE and S. FRAILE (Museo Nacional de Ciencias Naturales-CSIC, Madrid) and K. WOLF-SCHWENNINGER (Staatliches Museum für Naturkunde, Stuttgart). M. STACHOWITSCH (Biocenter, University Vienna) helped improve the English. We specifically thank the reviewers M. HARZHAUSER (Natural History Museum, Vienna) and W. WESSELS (Department of Earth Sciences, Utrecht University) for careful comments and critical remarks, and the editor A. KROH for helpful and necessary information. All these persons and institutions are gratefully acknowledged for their support.

References

- AYMARD, G. (1850): Mammifères fossiles des calcaires du Puys. – *Annales de la Société Agricul-ture, Sciences, Arts et Commerce du Puy*, **14**: 80–86.
- BÄRMANN, E.V. & RÖSSNER, G.E. (2011): Dental nomenclature in Ruminantia: Towards a stand-ard terminological framework. – *Mammalian Biology*, **76/6**: 762–768.
- BARONE, R. (1999): Anatomie comparée des mammifères domestiques. Tome 2. Arthrologie et myologie. 4^e édition. – pp. 760, Paris (Vigot).
- BECKER, D., ANTOINE, P.O., ENGESSER, B., HIARD, F., HOSTETTLER, B., MENKVELD-GFELLER, U., MENNECART, B., SCHERLER, L. & BERGER, J.P. (2010): Late Aquitanian mammals from Engehalde (Molasse Basin, Canton Bern, Switzerland). – *Annales de Paléontologie*, **96/3**: 95–116.
- BLONDEL, C. (1996): Les ongulés à la limite Eocène/Oligocène et au cours de l'Oligocène en Europe occidentale: analyses faunistiques, morpho-anatomiques et biogéochimiques ($\delta^{13}C$, $\delta^{18}O$). Implications sur la reconstitution des paléoenvironnements. – Unpublished PhD Thesis, University of Montpellier II, 103 pp.
- BLONDEL, C. (1997): Les ruminants de Pech Desse et de Pech du Fraysse (Quercy, MP 28); évolution des ruminants de l'Oligocène d'Europe. – *Geobios*, **30**: 573–591.
- BLONDEL, C. (1998): Le squelette appendiculaire de sept ruminants oligocènes d'Europe, impli-cations paléoécologiques. – *Comptes Rendus de l'Académie des Sciences de Paris*, **326**: 527–532.
- BLUMENBACH, J.F. (1779): *Handbuch der Naturgeschichte*. Theil 1. – xiii+448 pp., Göttingen (Johann Christian Dieterich).
- BODMER, R.D. (1990): Ungulate frugivores and the browser-graser continuum. – *Oikos*, **57**: 319–325.

- BOHLIN, B. (1946): The Fossil Mammals from the Tertiary Deposit of Taben-buluk, Western Kansu. Part II: Simplicidentata, Carnivora, Artiodactyla, Perissodactyla, and Primates. – In: The Sino-Swedish Expedition Publication, 28, VI. Vertebrate Palaeontology, 4. – *Palaeontologica Sinica*, new series C, **8B**: 1–259.
- BOWDICH, T.E. (1821): *An Analysis of the Natural Classification of Mammalia for the use of Students and Travellers.* – 115 pp., Paris (Smith).
- BRANDT J.F. (1855): Untersuchungen über die craniologischen Entwicklungsstufen und die davon herzuleitenden Verwandtschaften und Classificationen der Nager der Jetztwelt. p. 125–365. – In: BRANDT J.F. (ed.): *Beiträge zur näheren Kenntniss der Säugethiere Russlands.* – *Mémoires de l'Académie impériale des sciences de St. Pétersbourg*, Série 7: 1–365.
- BRUIJN DE, H., ÜNAY, E., SARAÇ, G. & YILMAZ, A. (2003): A rodent assemblage from the Eo/Oligocene boundary interval near Süngülü, Lesser Caucasus, Turkey. – *Coloquios de Paleontología*, **1**: 47–76.
- BUTLER, P.M. (1948): On the evolution of the skull and teeth in the Erinaceidae, with special reference to fossil material in the British Museum. – *Proceedings of the Zoological Society of London*, **118**: 446–500.
- DAXNER-HÖCK, G. (2001): New zapodids (Rodentia) from Oligocene-Miocene deposits in Mongolia. Part 1. – *Senckenbergiana lethaea*, **81/2**: 359–389.
- DAXNER-HÖCK, G., HÖCK, V., BADAMGARAV, D., FURTMÜLLER, G., FRANK, W., MONTAG, O. & SCHMID, H.-P. (1997): Cenozoic Stratigraphy based on a sediment-basalt association in Central Mongolia as Requirement for Correlation across Central Asia. – In: AGUILAR, J.P., LEGENDRE, S. & MICHAUX, J. (eds): *Biochronologie mammalienne du Cénozoïque en Europe et domaines reliés.* – *Mémoires et Travaux de l'Institut de Montpellier*, E.P.H.E., **21**: 163–176.
- DAXNER-HÖCK, G., BADAMGARAV, D. & MARIDET, O. (2014): Dipodidae (Rodentia, Mammalia) from the Oligocene and Early Miocene of Mongolia. – *Annalen des Naturhistorischen Museums in Wien, Serie A*, **116**: 131–214.
- DAXNER-HÖCK, G., BADAMGARAV, D. & MARIDET, O. (2015): Evolution of Tachyoryctoidinae (Rodentia, Mammalia): evidences of the Oligocene and early Miocene of Mongolia. – *Annalen des Naturhistorischen Museums in Wien, Serie A*, **117**: 161–195.
- DAXNER-HÖCK, G., BADAMGARAV, D., BARSBOLD, R., BAYARMAA, B., ERBAJEVA, M., GÖHLICH, U.B., HARZHAUSER, M., HÖCK, V., HÖCK, E., ICHINOROV, N., KHAND, Y., LÓPEZ-GUERRERO, P., MARIDET, O., NEUBAUER, T.A., OLIVER, A., PILLER, W.E., TSOGTBAATAR, K. & ZIEGLER, R. (2017): Oligocene Stratigraphy across the Eocene and Miocene boundaries in the Valley of Lakes (Mongolia). – In: DAXNER-HÖCK, G. & GÖHLICH, U.B. (eds): *The Valley of Lakes in Mongolia, a key area of Cenozoic mammal evolution and stratigraphy.* – *Palaeobiodiversity and Palaeoenvironments*, **97/1**: 111–218.
- DEMMENT, M.W. & SOEST VAN, P.J. (1985): A nutritional explanation for body-size patterns of ruminant and nonruminant herbivores. – *The American Naturalist*, **125**: 641–672.
- DEVYATKIN, E.B. (1981): The Cenozoic of Inner Asia (Stratigraphy, geochronology and correlation). – In: NIKIFOROVA, I. (ed.): *The Joint Soviet-Mongolian Scientific-Research, Geological Expedition, Transactions*, 27. – 196 pp., Moscow (Nauka). [in Russian]
- ENGESSER, B. (1980): Insectivora und Chiroptera (Mammalia) aus dem Neogen der Türkei. – *Schweizerische paläontologische Abhandlungen*, **102**: 45–149.
- ERBAJEVA, M.A. & DAXNER-HÖCK, G. (2014): The most prominent Lagomorpha from the Oligocene and early Miocene of Mongolia. – *Annalen des Naturhistorischen Museums in Wien, Serie A*, **116**: 215–245.

- ERBAJEVA, M.A. (2007): 5. Lagomorpha (Mammalia): preliminary results. – In: DAXNER-HÖCK, G. (ed.): Oligocene-Miocene vertebrates from the Valley of Lakes (Central Mongolia): Morphology, phylogenetic and stratigraphic implications. – *Annalen des Naturhistorischen Museums in Wien, Serie A*, **108**: 165–171.
- ERBAJEVA, M.A. & SEN, S. (1998): Systematic of some Oligocene Lagomorpha (Mammalia) from China. – *Neues Jahrbuch, Geologische Palaeontologische Monatshefte*, **2**: 95–105.
- FISCHER, G. (1814): *Zoognosia tabulis synopticis illustrata*. – xiv+465 pp., Moscow (Nicolai Sergei dis Vsevolozsky).
- FISCHER VON WALDHEIM, G. (1817): *Adversaria zoologica*. – *Mémoires de la Société Impériale des Naturalistes Moscou*, **5**: 357–472.
- FLOWER, W. (1883): On the Arrangement of the Orders and Families of Existing Mammalia. – *Proceedings of the Zoological Society of London*, **1883**: 178–186.
- GOMES RODRIGUES, H., MARIVAUX, L. & VIANEY-LIAUD, M. (2012a): The Cricetidae (Rodentia, Mammalia) from Ulanatal area (Inner Mongolia, China): new data concerning the evolution of Asian cricetids during the Oligocene. – *Journal of Asian Earth Sciences*, **56**: 160–179.
- GOMES RODRIGUES, H., MARIVAUX, L., & VIANEY-LIAUD, M. (2012b): Expansion of open landscapes in Northern China during the Oligocene induced by dramatic climate changes: paleoecological evidence. – *Palaeogeography, Palaeoclimatology, Palaeoecology*, **62–71**, 358–360.
- GRADSTEIN, F.M., OGG, J.G., SCHMITZ, M.D. & OGG, G.M. (2012): *The geologic time scale 2012*. – 2 vols, 1144 pp., Oxford (Elsevier).
- GRAY, J.E. (1821): On the natural arrangement of vertebrate animals. – *London Medical Repository*, **15/1**: 269–310.
- GREGORY, W.K. (1910): The orders of mammals. – *Bulletin of the American Museum of Natural History*, **37**: 1–524.
- GUREEV, A.A. (1960): Oligocene lagomorphs (Lagomorpha) from Mongoliaband Kazakhstan. – In: FLEROV, K.K. (ed.): *Tertiary Mammals*. – 5–34 pp., Moscow (Nauka Press). [in Russian]
- HARZHAUSER, M., DAXNER-HÖCK, G., ERBAJEVA, M.A., LÓPEZ-GUERRERO, P., MARIDET, O., OLIVER, A., PILLER, W.E., GÖHLICH, U.B. & ZIEGLER, R. (2017): Oligocene and early Miocene mammal biostratigraphy of the Valley of Lakes in Mongolia. – In: DAXNER-HÖCK, G. & GÖHLICH, U.B. (eds): *The Valley of Lakes in Mongolia, a key area of Cenozoic mammal evolution and stratigraphy*. – *Palaeobiodiversity and Palaeoenvironments*, **97/1**: 111–218.
- HARZHAUSER, M., DAXNER-HÖCK, G., LÓPEZ-GUERRERO, P., MARIDET, O., OLIVER, A., PILLER, W.E., RICHOS, S., ERBAJEVA, M.A., NEUBAUER, T.A. & GÖHLICH, U.B. (2016): Stepwise onset of the Icehouse world and its impact on Oligo-Miocene Central Asian mammals. – *Scientific Reports*, **6**: 36169. DOI: 10.1038/srep36169
- HÖCK, V., DAXNER-HÖCK, G., SCHMID, H.P., BADAMGARAV, D., FRANK, W., FURTMÜLLER, G., MONTAG, O., BARSBOLD, R., KHAND, Y. & SODOV, J. (1999): Oligocene-Miocene sediments, fossils and basalts from the Valley of Lakes (Central Mongolia) – an integrated study. – *Mitteilungen der Österreichischen Geologischen Gesellschaft*, **90** (1997): 83–125.
- HOFFSTETTER, R. & GASC, J.P. (1969): Vertebrae and ribs of modern reptiles. – In: GANS, C. (ed.): *Morphology A, Biology of the Reptilia*. – pp. 210–310, London & New York (Academic Press).
- HOU, L. (1984): The Aragonian vertebrate fauna of Xiacaswan, Jiangsu. 2. Aegypinae (Falconiformes, Aves). – *Vertebrata Palasiatica*, **22/1**: 14–19. [Chinese with English summary]

- HOU, L., ZHOU, Z., ZHANG, F. & LI, J. (2000): A new vulture from the Miocene of Shandong, eastern China. – *Vertebrata Palasiatica*, **38**: 104–110. [Chinese with English summary]
- HUANG, X. (1984): Fossil Erinaceidae (Insectivora, Mammalia) from the Middle Oligocene of Ulanatal, Alxa Zouqi, Nei Mongol. – *Vertebrata Palasiatica*, **22/4**: 306–309.
- HUANG, X.S. (1985): Middle Oligocene Ctenodactylids (Rodentia, Mammalia) of Ulanatal, Nei Mongol. – *Vertebrata Palasiatica*, **23/1**: 27–37. [Chinese with English summary]
- HUANG, X.S. (1992): Zapodidae (Rodentia, Mammalia) from the Middle Oligocene of Ulanatal, Nei Mongol. – *Vertebrata Palasiatica*, **30**: 249–286. [Chinese with English summary]
- HUTCHISON, J.H. (1974): Notes on type specimens of European Miocene Talpidae and a tentative classification of Old World Tertiary Talpidae (Insectivora: Talpidae). – *Geobios*, **7**: 211–256.
- JANIS, M. (1990): Correlation of cranial and dental variables with body size in ungulates and macropoids. – In: DAMUTH, J. & MAC-FADDEN, B.J. (eds): *Body Size of Mammalian Paleobiology: Estimating and Biological Implications*. – pp. 255–299, Cambridge (Cambridge University Press).
- KAUP, J.J. (1829): *Skizzirte Entwicklungs-Geschichte und natürliches System der europäischen Thierwelt*. – 203 pp., Darmstadt & Leipzig (Carl Wilhelm Leske).
- KÖHLER, M. (1993): Skeleton and Habitat of recent and fossil Ruminants. – *Münchner Geowissenschaftliche Abhandlungen, Serie A*, **25**: 1–88.
- KOSMA, R. (2004): The dentition of recent and fossil scincomorph lizard (Lacertilia, Squamata). – Systematics, functional morphology, palaeoecology, Fachbereich Geowissenschaften und Geographie, Universität Hannover, Hannover. – 187 pp., Hannover (Universität Hannover).
- KUROCHKIN, E.N. (1968a): Fossil remains of birds from Mongolia. – *Ornitologiya*, **9**: 323–330. [in Russian]
- KUROCHKIN, E.N. (1968b): New Oligocene birds from Kazakhstan. – *Paleontologicheskii Zhurnal*, **1**: 92–101. [in Russian]
- KUROCHKIN, E.N. (1976): A survey of Paleogene birds of Asia. – *Smithsonian Contributions to Palaeobiology*, **27**: 75–86.
- KUROCHKIN, E.N., LOPATIN, A.V. & ZELENKOV N.V. (2015): Fossil vertebrates of Russia and adjacent countries. Fossil Reptiles and Birds, Part 3. – 299 pp., Moscow (Russian Academy of Sciences Borissiak Paleontological Institute). [in Russian]
- LAURENTI, J.N. (1768): *Specimen medicum, exhibens synopsis reptilium emendatum cum experimentis circa venena et antidota Reptilium Austriacorum*. – 214 pp., Viennae (Typ. Joan. Thom. nob. de Trattner).
- LI, Q., GONG, Y.-X. & WANG, Y.-Q. (2017): New dipodid rodents from the Late Eocene of Erden Obo (Nei Mongol, China). – *Historical Biology*, **29**: 1–12.
- LINDSAY, E.H. (1978): *Eucricetodon asiaticus* (MATTHEW and GRANGER), an Oligocene rodent (Cricetidae) from Mongolia. – *Journal of Paleontology*, **52/3**: 590–595.
- LINNAEUS, C. (1758): *Systema naturae per regna tria naturae, secundum classes, ordines, genera, species, cum characteribus differentiis, synonymis, locis*, I. – 824 pp., Stockholm (Laurentii Salvii).
- LISKUN, I.G., & BADAMGARAV, D. (1977): Lithology of the Cenozoic of Mongolia. – The Joint Soviet-Mongolian Scientific-Research Geological Expedition, Transactions, **20**: 1–159. [in Russian]

- LOPATIN, A.V. (1999): New Early Miocene Zapodidae (Rodentia, Mammalia) from the Aral Formation of the Altynshokysu Locality (North Aral Region). – *Paleontological Journal*, **33/4**: 429–438.
- LOPATIN, A.V. (2002): The largest Asian *Amphexhinus* (Erinaceidae, Insectivora, Mammalia) from the Oligocene of Mongolia. – *Paleontological Journal*, **36/3**: 302–306.
- LÓPEZ MARTINEZ, N. (1989): Revisión sistemática y biostratigráfica de los Lagomorpha (Mammalia) del Terciario y Cuaternario de España. – *Memorias del Museo Paleontológico de la Universidad de Zaragoza*, **3**: 1–350.
- LÓPEZ-GUERRERO, P., MARIDET, O. & DAXNER-HÖCK, G. (2017a): Evolution of the genus *Eucricetodon* (Rodentia, Mammalia) from the Valley of Lakes (Mongolia): a taxonomical description and update on the stratigraphical distribution. – In: DAXNER-HÖCK, G. & GÖHLICH, U.B. (eds): *The Valley of Lakes in Mongolia, a key area of Cenozoic mammal evolution and stratigraphy*. – *Palaeobiodiversity and Palaeoenvironments*, **97/1**: 67–89.
- LÓPEZ-GUERRERO, P., MARIDET, O. & DAXNER-HÖCK, G. (2017b): Cricetidae (Rodentia, Mammalia) from the Oligocene of the Valley of Lakes (Mongolia): the genera *Aralocricetodon*, *Eocricetodon*, *Bagacricetodon*, *Witenia* and *Paracricetodon*. – In: DAXNER-HÖCK, G. & GÖHLICH, U.B. (eds): *The Valley of Lakes in Mongolia, a key area of Cenozoic mammal evolution and stratigraphy*. – *Palaeobiodiversity and Palaeoenvironments*, **97/1**: 93–109.
- MAITRE, E. (2014): Western European middle Eocene to early Oligocene Chiroptera: systematics, phylogeny and palaeoecology based on new material from the Quercy. – *Swiss Journal of Palaeontology*, **133**: 141–242.
- MANEGOLD, A., PAVIA, M. & HAARHOFF, P. (2014): A new species of *Aegyptius vulture* (Aegyptiinae, Accipitridae) from the early Pliocene of South Africa. – *Journal of Vertebrate Paleontology*, **34/6**: 1394–1407.
- MARIDET, O., WU, W.Y., YE, J., BI, S.D., NI, X.J. & MENG, J. (2009). *Eucricetodon* (Rodentia, Mammalia) from the Late Oligocene of the Junggar basin, Northern Xinjiang, China. – *American Museum Novitates*, **3665**: 1–21.
- MARTINEZ, J.-N. & SUDRE, J. (1995): The astragalus of Paleogene artiodactyls: comparative morphology, variability and prediction of body mass. – *Lethaia*, **28**: 197–209.
- MATTHEW, W.D. & GRANGER, W. (1923): Nine new Rodents from the Oligocene of Mongolia. – *American Museum Novitates*, **102**: 1–10.
- MATTHEW, W.D. & GRANGER, W. (1924): New insectivores and ruminants from the Tertiary of Mongolia, with remarks on the correlation. – *American Museum Novitates*, **105**: 1–7.
- MAYR, G. (2009): *Paleogene Fossil Birds*. – 262 pp., Heidelberg (Springer).
- MC KENNA, M.C. & HOLTON, C.P. (1967): A new Insectivore from the Oligocene of Mongolia and a new Subfamily of hedgehogs. – *American Museum Novitates*, **2311**: 1–22.
- MENNECART, B. (2012): The Ruminantia (Mammalia, Cetartiodactyla) from the Oligocene to the Early Miocene of Western Europe: systematics, palaeoecology and palaeobiogeography. – *GeoFocus*, **32**: 1–263.
- MENNECART, B. (2015): The European ruminants during the “*Microbunodon* Event” (MP28, latest Oligocene): impact of climate changes and faunal event on the ruminant evolution. – *PLoS One*, **10**: e0116830.
- MENNECART, B., BECKER, D. & BERGER, J.P. (2011): *Iberomeryx minor* (Mammalia, Artiodactyla) from the Early Oligocene of Soulce (Canton Jura, NW Switzerland): systematics and palaeodiet. – *Swiss Journal of Geosciences*, **104/Suppl. 1**: 115–132.

- MENNECART, B., BECKER, D. & BERGER, J.P. (2012a): Mandible shape of ruminants: between phylogeny and feeding habits. – In: MENDES, E.D. (ed.): *Ruminants: anatomy, behaviour and diseases*. – pp. 205–229, New York (Nova).
- MENNECART, B., GERAADS, D., SPASSOV, N. & ZAGORCHEV, I. (2018a): Discovery of the oldest European ruminant in the latest Eocene of Bulgaria: Did tectonics influence the diachronic development of the Grande Coupure? – *Palaeogeography, Palaeoclimatology, Palaeoecology*, **498**: 1–8.
- MENNECART, B., DE PERTHUIS, AD., RÖSSNER, G.E., GUZMÁN, J.A., PERTHUIS, A. & COSTEUR, L. (2018b): The first French tragulid skull (Mammalia, Ruminantia, Tragulidae) and associated tragulid remains from the Middle Miocene of Contres (Loir-et-Cher, France). Le premier crâne de Tragulidae français (Mammalia, Ruminantia) et les restes associés de Tragulidae du Miocène moyen de Contres (Loir-et-Cher, France). – *Comptes Rendus Palevol*, **17**/3: 189–200.
- MENNECART, B., SCHERLER, L., HIARD, F., BECKER, D. & BERGER, J.P. (2012 b): Ungulates from Rickenbach (type locality for MP29, Late Oligocene, Switzerland): palaeoecological and palaeoenvironmental implications. – *Swiss Journal of Palaeontology*, **131**: 161–181.
- MÉTAIS, G. & VISLOBOKOVA, I. (2007): Basal ruminants. – In: PROTHERO, D.R. & FOSS, S.E. (eds): *The evolution of artiodactyls*. – pp. 189–212, Baltimore (Johns Hopkins University Press).
- MÉTAIS, G., MENNECART, B. & ROOHI, G. (2017): A new assemblage of stem pecoran ruminants from the Oligocene Chitarwata Formation, Bugti Hills, Baluchistan, Pakistan: Palaeoenvironmental and paleobiogeographic implications. – *Journal of Asian Earth Sciences*, **136**: 40–49.
- MÉTAIS, G., WELCOMME, J.L. & DUCROCQ, S. (2009): New lophiomericyd ruminants from the Oligocene of the Bugti Hills (Balochistan, Pakistan). – *Journal of Vertebrate Paleontology*, **29**: 231–241.
- MONTGELARD, C., CATZEFLIS, F.M. & DOUZERY, E. (1997): Phylogenetic relationships of artiodactyls and cetaceans as deduced from the comparison of cytochrome b and 12S rRNA mitochondrial sequences. – *Molecular Biology and Evolution*, **14**/5: 550–559.
- MUIZON DE, C. (1977): Revision des lagomorphes des couches a Baluchitherium (Oligocene supérieur) de San-tao-ho (Ordos, Chine). – *Bulletin de Museum National d’Histoire Naturelle, Section Science de la Terre*, **65**: 265–294.
- NOVELLO, A., BLONDEL, C. & BRUNET, M. (2010): Feeding behavior and ecology of the Late Oligocene Moschidae (Mammalia, Ruminantia) from La Milloque (France): Evidence from dental microwear analysis. – *Comptes Rendus Palevol*, **9**: 471–478.
- NOWAK, R.M. (1999): *Walker’s mammals of the world*, vol. 2 (6th edition). – 1936 pp., Baltimore and London (John Hopkins University Press).
- OLIVER, A. & DAXNER-HÖCK, G. (2017): Large-sized species of Ctenodactylidae from the Valley of Lakes (Mongolia): an update of dental morphology, biostratigraphy and paleobiogeography. – *Paleontologia electronica*, **20.1/A**: 1–22.
- OLIVER, A., SANISIDRO, O., BAYARMAA, B., ICHINNOROV, N. & DAXNER-HÖCK, G. (2017): Diversification rates in Ctenodactylidae (Rodentia, Mammalia) from Mongolia. – In: DAXNER-HÖCK, G. & GÖHLICH, U.B. (eds): *The Valley of Lakes in Mongolia, a key area of Cenozoic mammal evolution and stratigraphy*. – *Palaeobiodiversity and Palaeoenvironments*, **97**/1: 51–65.
- OLSON, S.L. (1985): The fossil record of birds. – In: FARNER, D.S., KING, J.R. & PARKES, K.C. (eds): *Avian Biology*, **8**. – pp. 79–238, New York (Academic Press).
- OPPEL, M. (1811): *Die Ordnungen, Familien und Gattungen der Reptilien als Prodrom einer Naturgeschichte derselben*. – 87 pp., München (Joseph Lindauer).

- PAUZER, A.A. (1987): The report of 1:200.000 scale geological mapping in the south-eastern part of the Mongolian Altai. – No. 4186. Ulaanbaatar (State Geological Fund of Mineral Resources and Petroleum Authority of Mongolia). [in Russian]
- REUMER, J.W.F. (1984): Ruscinian and early Pleistocene Soricidae (Insectivora, Mammalia) from Tegelen (The Netherlands) and Hungary. – *Scripta Geologica*, **73**: 1–173.
- REUMER, J.W.F. (1987): Redefinition of the Soricidae and the Heterosoricidae (Insectivora, Mammalia) with the description of the Crocidososoricinae, a new family of the Soricidae. – *Revue de Paléobiologie*, **6/2**: 189–192.
- SCHAUB, S. (1930): Fossile Sizistinae. – *Eclogae geologicae Helvetiae*, **23/2**: 616–636.
- SCHERLER, L., MENNECART, B., HIARD, F. & BECKER, D. (2013): Evolution of terrestrial hoofed-mammals during the Oligocene-Miocene transition in Europe. – *Swiss Journal of Geosciences*, **106**: 349–369.
- SCHMIDT-KITTLER, N., VIANEY-LIAUD, M. & MARIVAUX, L. (2006): 6. The Ctenodactylidae (Rodentia, Mammalia). – In: DAXNER-HÖCK, G. (ed.): *Oligocene-Miocene Vertebrates from the Valley of Lakes (Central Mongolia): Morphology, phylogenetic and stratigraphic implications*. – *Annalen des Naturhistorischen Museums Wien, Serie A*, **108**: 173–215.
- SCOPOLI, G.A. (1777): *Introductio ad historiam naturalem sistens genera lapidum, plantarum, et animalium: hactenus detecta, characteribus essentialibus donata, in tribus divisa, subinde ad leges naturae*. – pp. 540, Prag (Wolfgang Gerle).
- SCOTT, K.M. (1990): Postcranial dimensions of ungulates as predictors of body mass. – In: DAMUTH, J. & MAC-FADDEN, B.J. (eds): *Body Size of Mammalian Paleobiology: Estimating and Biological Implications*. – pp. 301–335, Cambridge (Cambridge University Press).
- SIGÉ, B. (1968): Les chiroptères du Miocène inférieur de Bouzigues. I. Étude systématique. – *Palaeovertebrata*, **1/3**: 65–133.
- SUDRE, J. (1984): *Cryptomeryx* SCHLOSSER, 1886, tragulidé de l'Oligocène d'Europe; relations du genre et considérations sur l'origine de ruminants. – *Palaeovertebrata*, **14**: 1–31.
- SUN, J. & WINDLEY, B.F. (2015): Onset of aridification by 34 Ma across the Eocene-Oligocene transition in Central Asia. – *Geology*, **11**: 1015–1018.
- TEILHARD DE CHARDIN, P. (1926): Description des mammifères tertiaires de Chine et de Mongolie. – *Annales de Paléontologie*, **15**: 1–52.
- THALER, L. (1966): Les rongeurs fossiles du Bas-Languedoc dans leurs rapports avec l'histoire des faunes et la stratigraphie du Tertiaire d'Europe. – *Mémoires du Muséum National d'Histoire Naturelle, Series C*, **17**: 1–295.
- THOMAS, O. (1897): On the genera of rodents: an attempt to bring up to date the current arrangement of the order. – *Proceedings Zoological Society London*, **1897**: 1012–1028.
- VIANEY-LIAUD, M., SCHMIDT-KITTLER, N. & MARIVAUX, L. (2006): The Ctenodactylidae (Rodentia) from the Oligocene of Ulanatal (Inner Mongolia, China). – *Palaeovertebrata*, **34/3–4**: 111–206.
- VIEILLOT, L.J.P. (1816): *Analyse d'une nouvelle ornithologie élémentaire*. – 70 pp., Paris (Deterville).
- VISLOBOKOVA, I.A. (1997): Eocene-Early Miocene ruminants in Asia. – In: AGUILAR, J.P., LEGENDRE, S. & MICHAUX, J. (eds): *Biochronologie mammalienne du Cénozoïque en Europe et domaines reliés*. – *Mémoires et Travaux de l'Institut de Montpellier, E.P.H.E.*, **21**: 215–223.

- VISLOBOKOVA, I. & DAXNER-HÖCK, G. (2002): Oligocene-Early Miocene Ruminants from the Valley of Lakes (Central Mongolia). – *Annalen des Naturhistorischen Museums in Wien, Serie A*, **103**: 213–235.
- WANG, B.Y. (1985): Zapodidae (Rodentia, Mammalia) from the Lower Oligocene of Qujing, Yunnan, China. – *Mainzer geowissenschaftliche Mitteilungen*, **14**: 345–367.
- WANG, B.Y. (1997): The Mid-Tertiary Ctenodactylidae (Rodentia, Mammalia) of eastern and central Asia. – *Bulletin of the American Museum of Natural History*, **234**: 1–88.
- WANG, B.Y. (2003): Dipodidae (Rodentia, Mammalia) from the mid-tertiary deposits in Danghe area, Gansu, China. – *Vertebrata PalAsiatica*, **41/2**: 89–103. [Chinese with English summary]
- WANG, B.Y. & QIU Z.X. (2000): Dipodidae (Rodentia, Mammalia) from the Lower Member of Xianshuihe Formation in Lanzhou Basin, Gansu, China. – *Vertebrata PalAsiatica*, **38/1**: 10–35. [Chinese with English summary]
- WESSELS, W., BADAMGARAV, D., VAN OLSELEN, V. & DAXNER-HÖCK, G. (2014): Tsaganomyidae (Rodentia, Mammalia) from the Oligocene of Mongolia (Valley of Lakes). – *Annalen des Naturhistorischen Museums in Wien, Serie A*, **116**: 293–325.
- ZANAZZI, A. & KOHN, M.J. (2008): Ecology and physiology of White River mammals based on stable isotope ratios of teeth. – *Palaeogeography, Palaeoclimatology, Palaeoecology*, **257**: 22–37.
- ZELENKOV, N.V. (2016): Evolution of bird communities in the Neogene of Central Asia, with a review of the Neogene fossil record of Asian birds. – *Paleontological Journal*, **50/12**: 1421–1433.
- ZIEGLER, R. (2000): The bats (Chiroptera, Mammalia) from the Late Oligocene Fissure Fillings Herrlingen 8 and Herrlingen 9 near Ulm (Baden-Württemberg). – *Senckenbergiana lethaea*, **80/2**: 647–683.
- ZIEGLER, R. (2003): *Myotis horaceki* pro *Myotis intermedius* ZIEGLER 2000 (Chiroptera, Mammalia) (=non *Myotis bechsteini intermedius* RYBÁR 1976). – *Senckenbergiana lethaea*, **83/1–2**: 2.
- ZIEGLER, R., DAHLMANN, T. & STORCH, G. (2007): 4. Marsupialia, Erinaceomorpha and Soricomorpha (Mammalia). – In: DAXNER-HÖCK, G. (ed.): Oligocene-Miocene Vertebrates from the Valley of Lakes (Central Mongolia): Morphology, phylogenetic and stratigraphic implications. – *Annalen des Naturhistorischen Museums Wien, Serie A*, **108**: 53–164.
- ZITTEL, K.A. (1893): *Handbuch der Paläontologie*. I. Abtheilung: Paläozoologie. IV. Band Vertebrata (Mammalia). – xi+799 pp., München & Leipzig (R. Oldenbourg).